NASA TECHNICAL NOTE

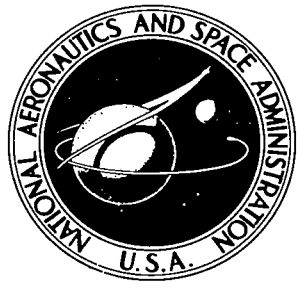

NASA TN D-6470
C.1

NASA TN D-6470

CLOUD COMPARISONS BETWEEN APOLLO 6 PHOTOGRAPHY AND ATS 3 AND ESSA 3 PHOTOGRAPHY

by William E. Shenk

Goddard Space Flight Center
Greenbelt, Md. 20771

NATIONAL AERONAUTICS AND SPACE ADMINISTRATION • WASHINGTON, D. C. • OCTOBER 1971

1. Report No.	2. Government Accession No.	3. Recipient's Catalog No.
NASA TN D-6470		

4. Title and Subtitle	5. Report Date
Cloud Comparisons Between Apollo 6 Photography and ATS 3 and ESSA 3 Photography	September 1971
	6. Performing Organization Code
7. Author(s)	8. Performing Organization Report No.
William E. Shenk	G-1040
9. Performing Organization Name and Address	10. Work Unit No.
Goddard Space Flight Center Greenbelt, Maryland 20771	11. Contract or Grant No.
	13. Type of Report and Period Covered
12. Sponsoring Agency Name and Address	Technical Note
National Aeronautics and Space Administration Washington, D.C. 20546	14. Sponsoring Agency Code

15. Supplementary Notes

16. Abstract

Concurrent data obtained via ATS 3 and ESSA 3 and from Apollo 6 high-resolution photography are compared. The spatial-resolution ratio between the Apollo 6 data and the data from the other satellites is about 50:1. Though the original ATS 3 cloud cover estimates are 13 to 14 percent higher than the Apollo 6 estimates (primarily in areas of low cumuliform clouds), corrections for the viewing perspective and spatial resolution bring the former estimates to within 5 percent of the latter. These results tend to confirm recent calculations made from satellite measurements of about 30 percent for the earth albedo. Cloud cover estimates made from the ESSA 3 satellite data are lower than the concurrent Apollo 6 data.

Cloud type distributions are obtained via normal and stereographic viewing of Apollo 6 picture pairs for a strong midlatitude cold front and for tropical and subtropical regions. Most of the cloudiness is shown to be either high or low, with middle cloudiness confined to large, organized weather systems.

17. Key Words Suggested by Author	18. Distribution Statement
Percentage of Cloud Cover Cloud Type Distributions Spatial Resolution Earth Albedo	Unclassified–Unlimited

19. Security Classif. (of this report)	20. Security Classif. (of this page)	21. No. of Pages	22. Price
Unclassified	Unclassified	47	$3.00

*For sale by the National Technical Information Service, Springfield, Virginia 22151

CONTENTS

CLOUD COMPARISONS BETWEEN APOLLO 6 PHOTOGRAPHY AND ATS 3 AND ESSA 3 PHOTOGRAPHY

by
William E. Shenk
Goddard Space Flight Center

1. INTRODUCTION

Within the past decade, a concerted effort has been made to map globally the cloud cover over the earth using the data obtained from meteorological satellites. In addition, many researchers continue to improve their understanding of cloud cover observations made by the large network of surface stations by comparing this information with data recorded by meteorological satellites, aircraft flights, and sunshine recorders.

The three fundamental factors affecting the accurate measurement of cloud cover are the spatial resolution, the brightness or thermal contrast between a cloud and the background, and the viewing perspective. A surface observer has no difficulty with brightness contrast (except for thin cirrus, especially with a haze background) nor with spatial resolution, but he views a substantial portion of the sky at an elevation angle that is less than or equal to 30 deg. As a result, he sees the sides of the clouds as well as the cloud bases, and an overestimate of cloud cover is often made. The perspective becomes especially important when the cloud thickness exceeds the cloud width. Young (1967) found that there was a natural tendency for observers to overestimate cloud amounts when simulated cloud patterns with known cloud covers were used.

The perspective effect has been examined by a number of investigators. To estimate the probability of clear lines of sight, Lund (1965) developed a cloud model that considered cloud width, thickness, and spacing. His results indicated the importance of viewing angle (e.g., at Tampa, Florida, the probability of a clear line of sight for August cloud cover was about 20 percent greater when the clouds were viewed straight down than when they were viewed at an elevation angle of 22 deg). In a later paper, Lund (1966) assessed five different methods for estimating clear lines of sight and demonstrated the significance of perspective on each. Some of these methods were developed by Fox (1961) and McCabe (1965). Appleman (1962) reported a 16 percent overestimation of cloud cover in ground observations of partly cloudy sky cover conditions compared with simultaneous aircraft measurements. Bertoni (1970) noted similar perspective effects with aircraft observations of cloud and haze free lines of sight at different elevation angles.

If cloud cover estimates are to be made from visible or infrared measurements received via a meteorological satellite, the receiving instrument must have sufficient sensitivity to detect the different levels of terrestrial energy reflected or emitted from the cloud and the adjacent background. Instrument sensitivity has steadily improved during the lifetime of the meteorological satellite program.

The routine viewing of the cloud cover over the earth (in the visible) has been accomplished with the vidicon camera (Schwalb and Gross, 1969), which was first launched in 1960 on TIROS 1. However, vidicon-camera outputs are affected by internal temperature changes as well as electronics degradation and residual images. Also, data-processing techniques have injected other uncertainties into the final product. Radiometers and line-scan cameras with improved dynamic ranges and sensitivities have been flown experimentally and are replacing the vidicon camera. Thus, high quality visible measurements from sensitive instrumentation are becoming routinely available.

An example of a successful instrument with high sensitivity and greater dynamic range than the vidicon camera is the spin-scan camera flown on the geosynchronous satellites ATS 1 and ATS 3. This camera made recordings of reflected visible light with photomultiplier detectors. The earth was viewed at 1/2-hr intervals; thus, normalized brightness measurements can be used to study the daylight portion of diurnal fluctuations in cloud cover.

The remaining fundamental factor, sensor spatial resolution, has received only limited quantitative investigation. If the spatial resolution is insufficient to resolve individual cloud elements or holes in an extensive cloud deck, the result is a smearing of the cloud patterns and an overestimation of the cloud cover. Erickson and Hubert* qualitatively illustrated this effect with a number of cases of small-scale cloudiness viewed by the wide- and narrow-angle cameras on TIROS 1. The spatial resolutions of these cameras were 4 and 0.4 km, respectively. From their work with simulated cloud patterns, Shenk and Salomonson (1971) concluded that the spatial resolution is important if the ratio of the areal cloud size to the areal resolution element size of the sensor is less than 100. The results from the simulated cloud patterns were verified with real cloud patterns. When compared with the perspective, the spatial resolution can be especially important for satellite measurements because information gathered by the satellite at local zenith angles greater than ±60 deg is often not used. In fact, although perspective viewing remains an important consideration for the satellite data, this factor should not be as significant as it is for the surface observer whose range of zenith angles extends to ±80 deg or more.

Cloud cover charts with varying spatial and temporal resolutions have been prepared by numerous investigators from the abundance of available satellite data. A synopsis of these investigations has been written by Salomonson.** Other researchers have compared satellite measurements with conventional surface cloud observations to determine the relationships between the two and have found, in general, that the cloud cover estimates obtained from both are reasonably similar. However, overestimates of the percentage of cloud cover could be made from both kinds of observations, due to the perspective for the surface data and the resolution for the satellite data. The satellite estimates are usually lower than the surface-observation estimates (see Barnes, 1966). Explanations for this include increased perspective for the ground observer, insufficient instrument sensitivity to detect cumulus cloud fields where a small percent of the earth is covered by clouds, and data processing methods used for the nephanalyses.

*Erickson, C. O., and L. F. Hubert, 1961: "Identification of Cloudforms from TIROS I Pictures", United States Weather Bureau MSL Report 7, United States Weather Bureau, Washington, D.C., 68 pp.

**Salomonson, V. V., 1969: "Cloud Statistics in Earth Resources Technology Satellite (ERTS) Mission Planning", NASA—Goddard Space Flight Center Document X-622-69-386, Goddard Space Flight Center, Greenbelt, Maryland, 19 pp.

It is probable that neither the meteorological satellite data (generally with about 4-km sensor spatial resolution) nor surface observations provide accurate cloud cover estimates for all cloud types and sizes. Observations are required from an instrument on a platform sufficiently high above the earth to minimize the effect of perspective and with sufficient spatial resolution and sensitivity to detect and define the areal extent of all the clouds that are present. Currently, there is no meteorological satellite spacecraft system that meets the above criteria. However, on April 4, 1968, a color camera on the unmanned Apollo 6 spacecraft took a series of high-resolution overlapping photographs with the camera pointing nearly straight down for portions of two orbits. The combination of sensitive film, high spatial resolution, and the location of the camera high enough above the earth to photograph an extensive area with small perspective differences satisfied the basic requirements for accurate cloud cover observations. Thus, this set of Apollo photographs can be used to determine accurate cloud cover and type distributions that provide precise information that can be compared with observations from other sources. Such comparisons then can be used to investigate what normalization is needed for cloud observations from sources for which data were taken concurrently with the Apollo photographs. In this study, the concomitant satellite data were acquired from the ESSA 3 and ATS 3 satellites.

2. THE APOLLO 6, ATS 3, AND ESSA 3 DATA

The color photographs taken by the Mariner 220-G 70-mm sequence camera on the Apollo 6 spacecraft had a spatial resolution of approximately 30 meters. With a constant picture interval of 8.64 seconds, adjacent pictures had an overlap of about 55 percent, which permitted the entire photographed area to be viewed stereographically.

Two segments from the total Apollo photographic sequence were chosen for analysis. Figure 1 depicts the position of these segments relative to the position of the ATS 3 geosynchronous satellite for which the subsatellite point was 84° W. The other portions of the Apollo 6 photography were taken at night or at times when there were no concurrent satellite data available or at positions where clouds were absent. The first segment of the photography, frames 836 to 935, showed clouds associated with subtropical and tropical weather; the second segment, frames 1464 to 1510 (taken in the following orbit), traversed a strong midlatitude cold-frontal structure and some subtropical cloudiness not far from the beginning of the first segment.

The three-channel Multicolor Spin-Scan Color Camera (MSSCC) was carried on the ATS 3 geosynchronous satellite as a meteorological instrument. This camera records reflected visible light via three photomultiplier detectors. Most of the data received from this instrument have come from the 0.48 to 0.58 μm (green) channel; the data from that channel were available on April 4, 1968. The subsatellite-point spatial resolution of the MSSCC was 3.7 km. (A more complete description of the MSSCC can be found in GSFC, 1968, and Stamm and Vonder Haar, 1970.)

The ATS 3 data are available in digital form (magnetic tape) or analog form (photographic print or magnetic tape). For this study, full earth photographs were generated when the data were projected onto film from a photofacsimile recorder. Black-and-white photographs of sectors of the earth's surface were produced from digital data expanded by a factor of 4 and then photographed in the same manner as for the full-earth-disk photographs. Hereafter, the full-earth photographs will be referred to as "1X" ATS photographs and the regional photographs as "4X" photographs.

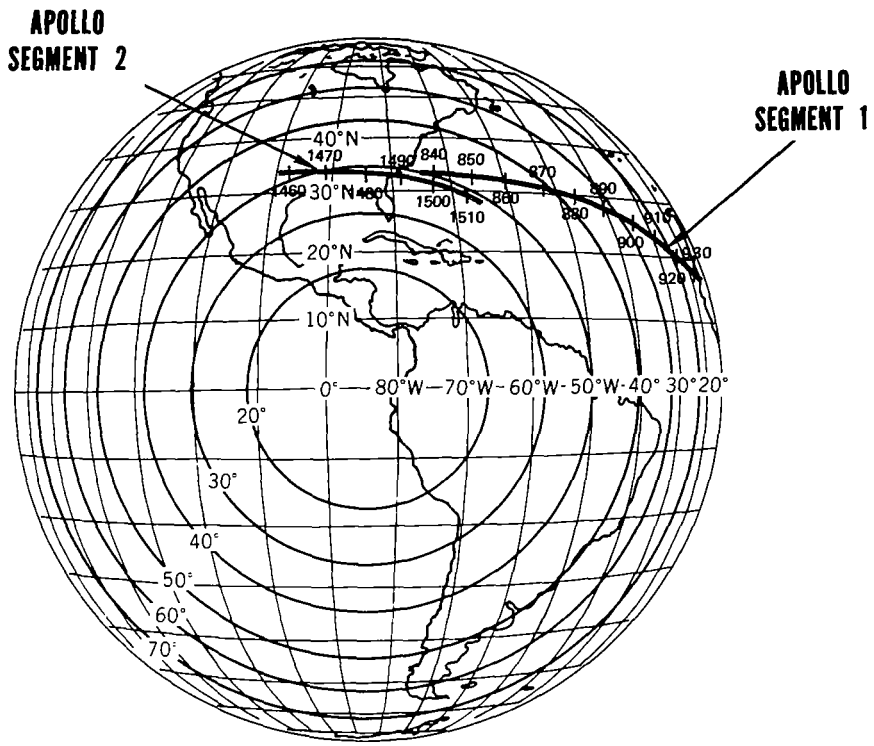

Figure 1—The subsatellite track of Apollo 6 over the regions covered by Apollo segments 1 and 2, as seen from the location of the ATS 3 geosynchronous satellite on April 4, 1968. The concentric circles with the subsatellite point at their centers are isolines of local zenith angle.

Figures 2 and 3 illustrate the 1X and 4X photographs, respectively, for April 4, 1968, close to the time when segment 1 of the Apollo 6 data was taken. The area common to both pictures is the upper right quadrant of the 1X photograph. Differences in detail, due most likely to the photographic printing process, are clearly visible between the two pictures. Area *A* in the 1X picture shows some cellular cloud structure, while the same area in the 4X picture reveals considerable cellular structure.

The data from the polar-orbiting, sun-synchronous ESSA 3 satellite were obtained with a 1-inch vidicon camera mounted on the satellite (Environmental Data Service, 1967). In addition to the standard black-and-white photographic output, the measurements were available in digitized-mosaic form. Figures 4 and 5 show examples of a routine photograph and a photographic representation of the digital mosaic, respectively, near the time when Apollo segment 1 was photographed. The region common to both photographs extends from the West African Coast westward for about 20 deg. Since the resolutions of the two data displays are comparable, the information contents of the two look similar.

Table 1 lists the times that information was gathered from Apollo 6, ATS 3, and ESSA 3 for the two Apollo segments. As can be seen in the table, at no point along the Apollo 6 track was the Apollo data taken more than 16 minutes from the data acquired by the other platforms. The 16-minute

Figure 2—ATS 3 1X, 8X10 photographic print 11G taken on April 4, 1968. The end-of-frame time was 1359:10 GMT.

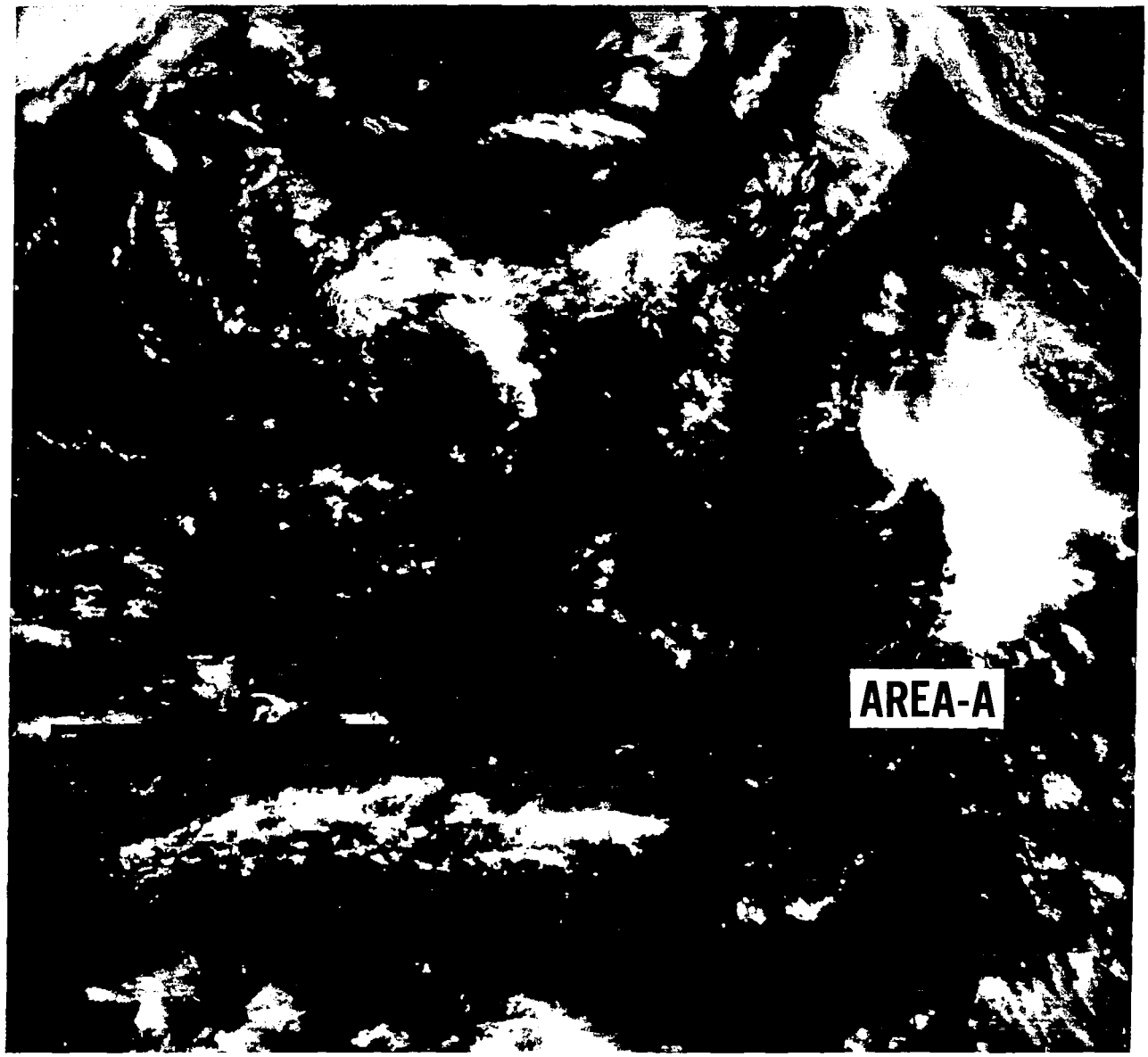

Figure 3—ATS 3 4X digital enlargement 8X10 photographic print which covers a portion of the nearly full-earth disk shown in Figure 2.

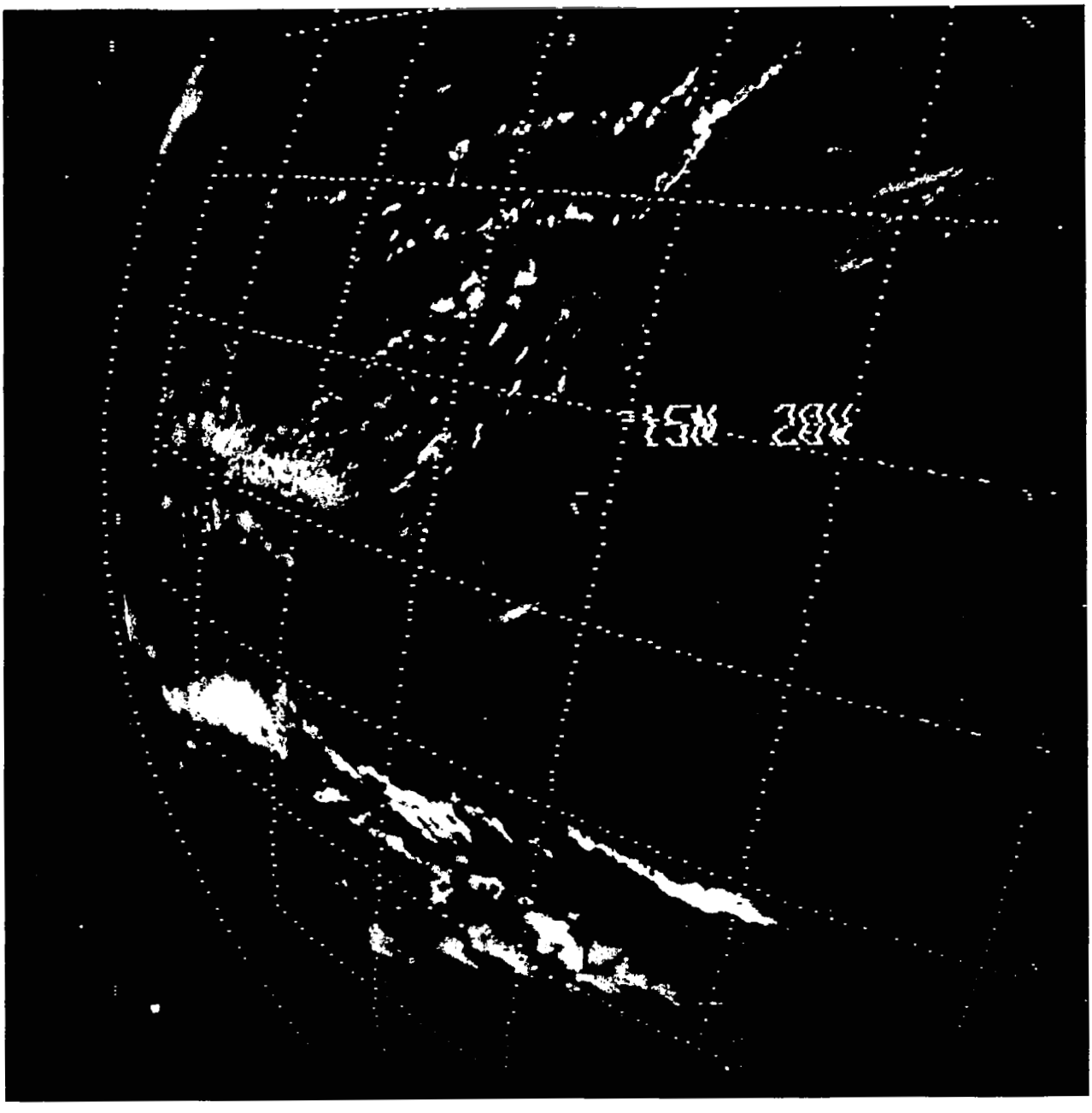

Figure 4—A photograph from ESSA 3 (frame 6) taken during orbit 6909 at 1338 GMT (15° N, 20° W).

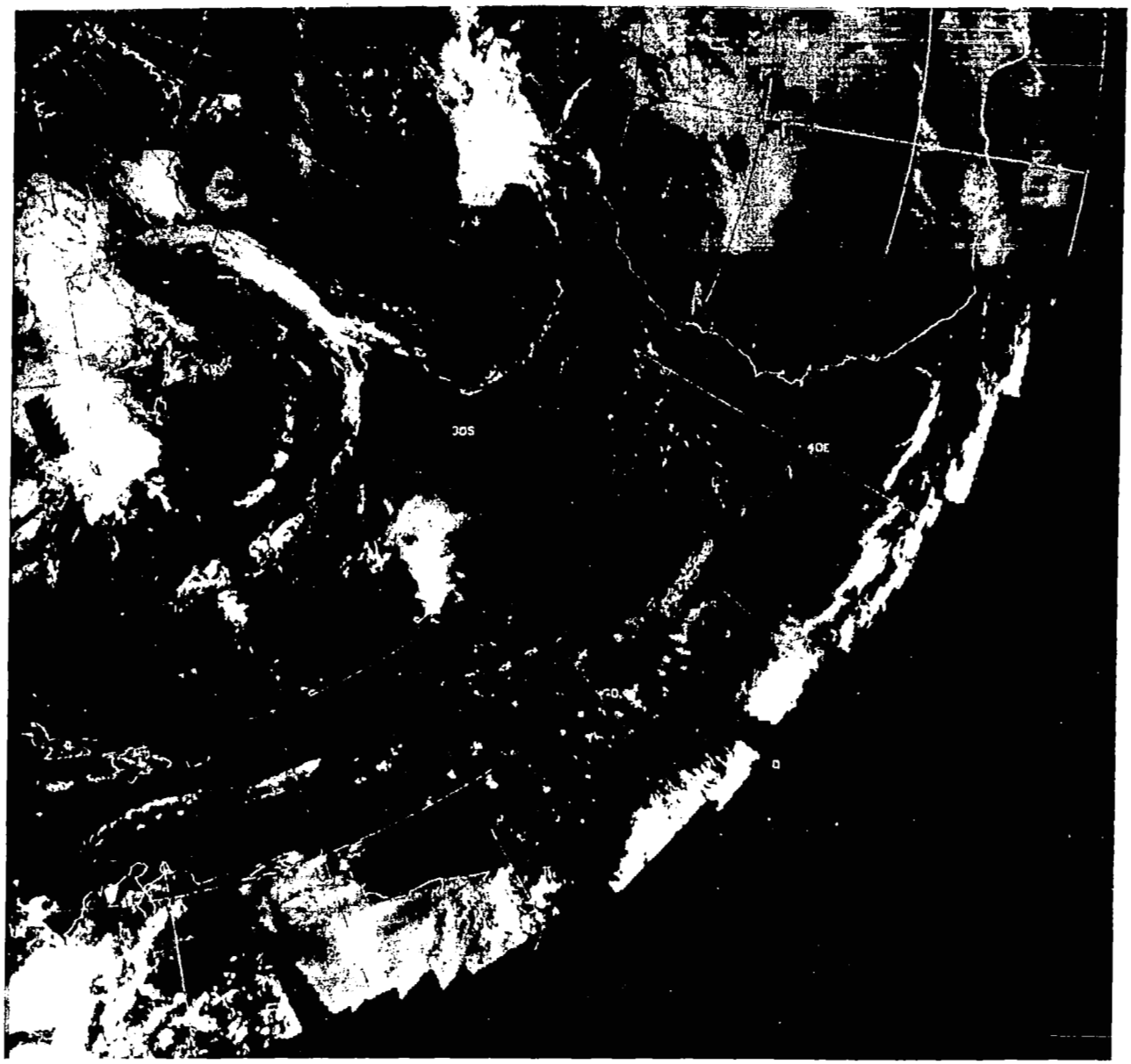

Figure 5—Photographic representation of a digitized mosaic prepared from ESSA 3 brightness measurements of April 4, 1968 (composite passes 6907 through 6919).

Table 1—The times (GMT) on April 4, 1968, when concurrent measurements were acquired from Apollo 6, ATS 3, and ESSA 3 for each Apollo segment.

Spacecraft	Apollo segment 1 (frames 836-935)	Apollo segment 2 (frames 1464-1510)
Apollo 6	1340 to 1354	1512 to 1519
ATS 3	1344 to 1349	1508 to 1510
ESSA 3	1338 to 1342	–

separation occurred between the Apollo 6 and ESSA 3 data at the extreme eastern end of Apollo segment 1, whereas the ATS 3 and Apollo 6 measurements were never taken more than 9 minutes apart. Therefore, direct individual cloud comparisons were possible for the data received from the three satellites. The ESSA 3 camera viewed the area covered by the rest of Apollo segment 1 and all of Apollo segment 2 about 2 to 4 hours after the Apollo 6 photography was taken, which was not close enough in time to the Apollo 6 information to allow its use.

It was recognized that differences in photographic processing could affect cloud type interpretation and cloud cover calculations. As a result, prints with different contrasts were made for the ATS 3 and ESSA 3 data to examine any such effects. This attempt produced slight differences, particularly in apparent cloud brightness, that would mostly affect cloud type identification; however, the differences were considered to be too insignificant to require other methods of data analysis.

3. THE METEOROLOGICAL SITUATION

Figures 6 and 7 show the National Meteorological Center (NMC) surface and 500-mb analyses, respectively, at 1200 GMT on April 4, 1968, for the western portion of Apollo segment 1. The Apollo 6 path crossed and recrossed a weak stationary front in the western Atlantic. This front was deleted from the NMC analysis 6 hours later. There is no evidence of a surface disturbance along the portion of the front that was viewed in the Apollo photography. There was a pronounced 500-mb trough on the 1200 GMT map with a possibility of a closed circulation at 29° N, 57° W. The evidence for a 500-mb closed circulation was not as great 12 hours later. To the east of 45° W along the Apollo track, the synoptic pattern was devoid of fronts or closed circulations at any tropospheric level, and, therefore, the charts for this region are not presented. Thus, the synoptic pattern was weak, with mesoscale circulations being the dominant circulation pattern over most of segment 1. A different synoptic situation was associated with segment 2. A double cold-frontal structure, which Apollo 6 crossed in the lower Mississippi Valley, was analyzed in the eastern third of the United States. This can be seen in the NMC North American surface chart at 1500 GMT, which is shown in Figure 8. Thus, the cloud regimes viewed within each Apollo segment were produced by markedly different weather patterns, and, because of this, the data comparisons within each segment were analyzed separately.

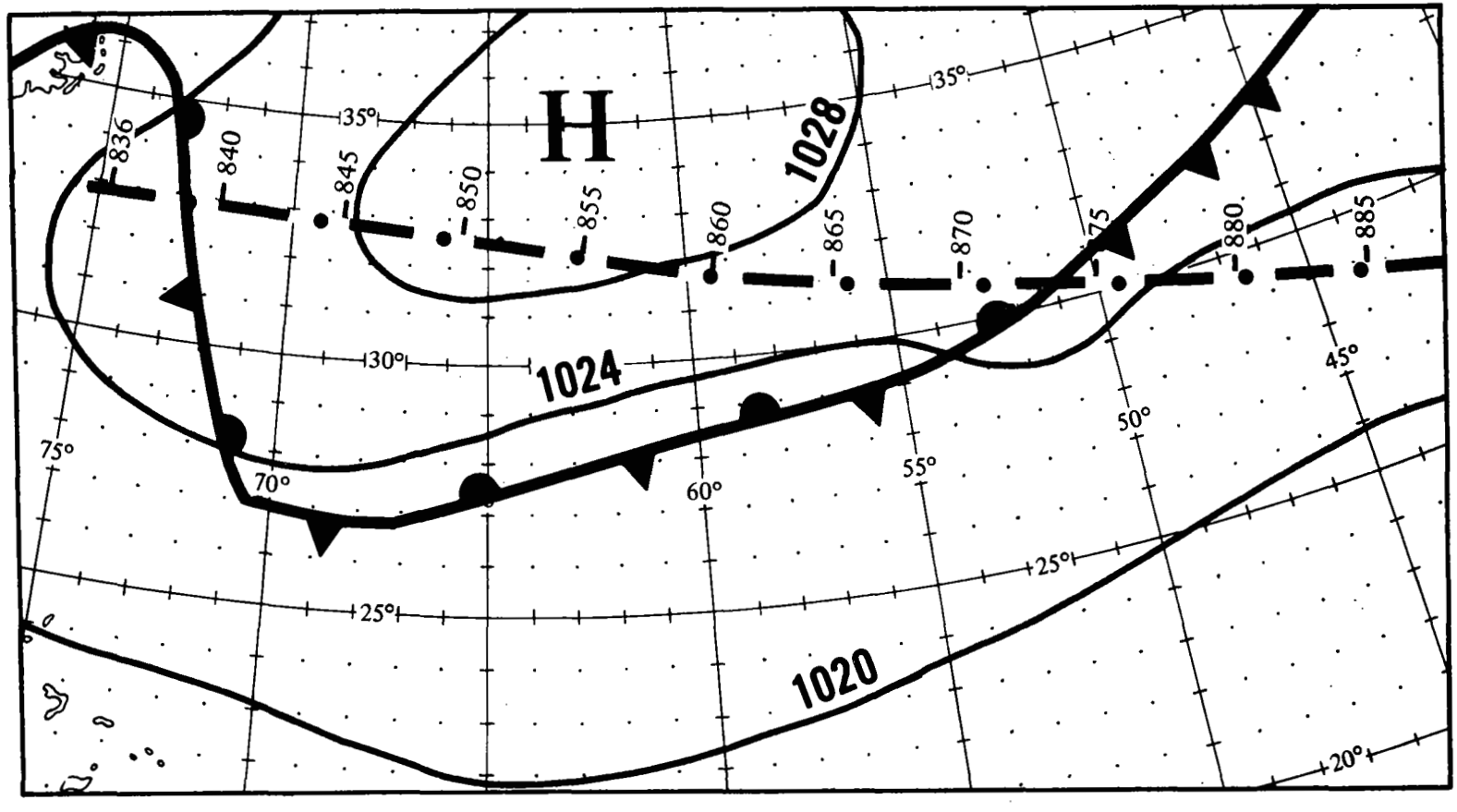

Figure 6—NMC surface analysis at 1200 GMT, April 4, 1968. The dot-dash line indicates the Apollo 6 subsatellite track, with the Apollo frame numbers shown above the track.

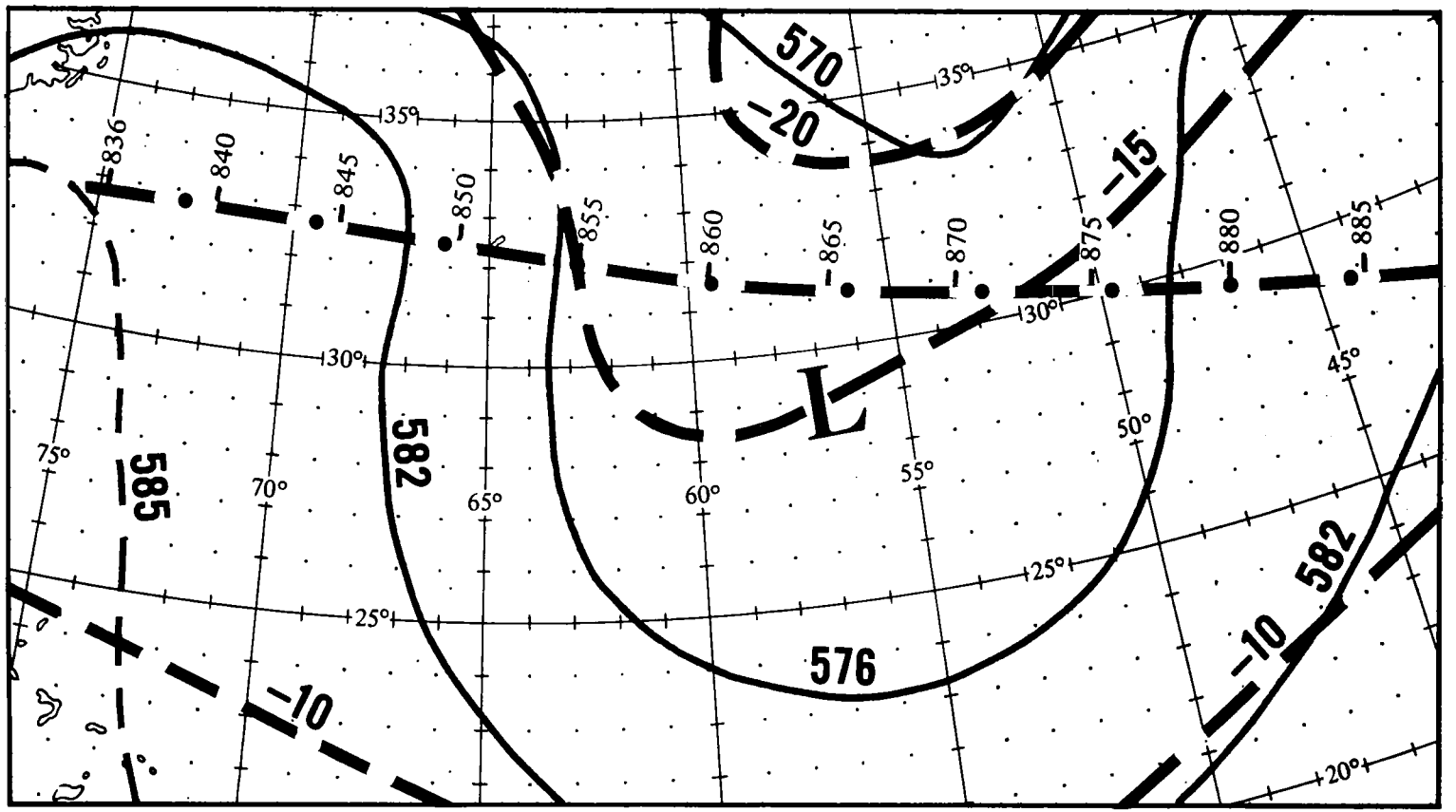

Figure 7—NMC 500-mb analysis at 1200 GMT, April 4, 1968. The dot-dash line indicates the Apollo 6 subsatellite track, with the Apollo frame numbers shown above the track.

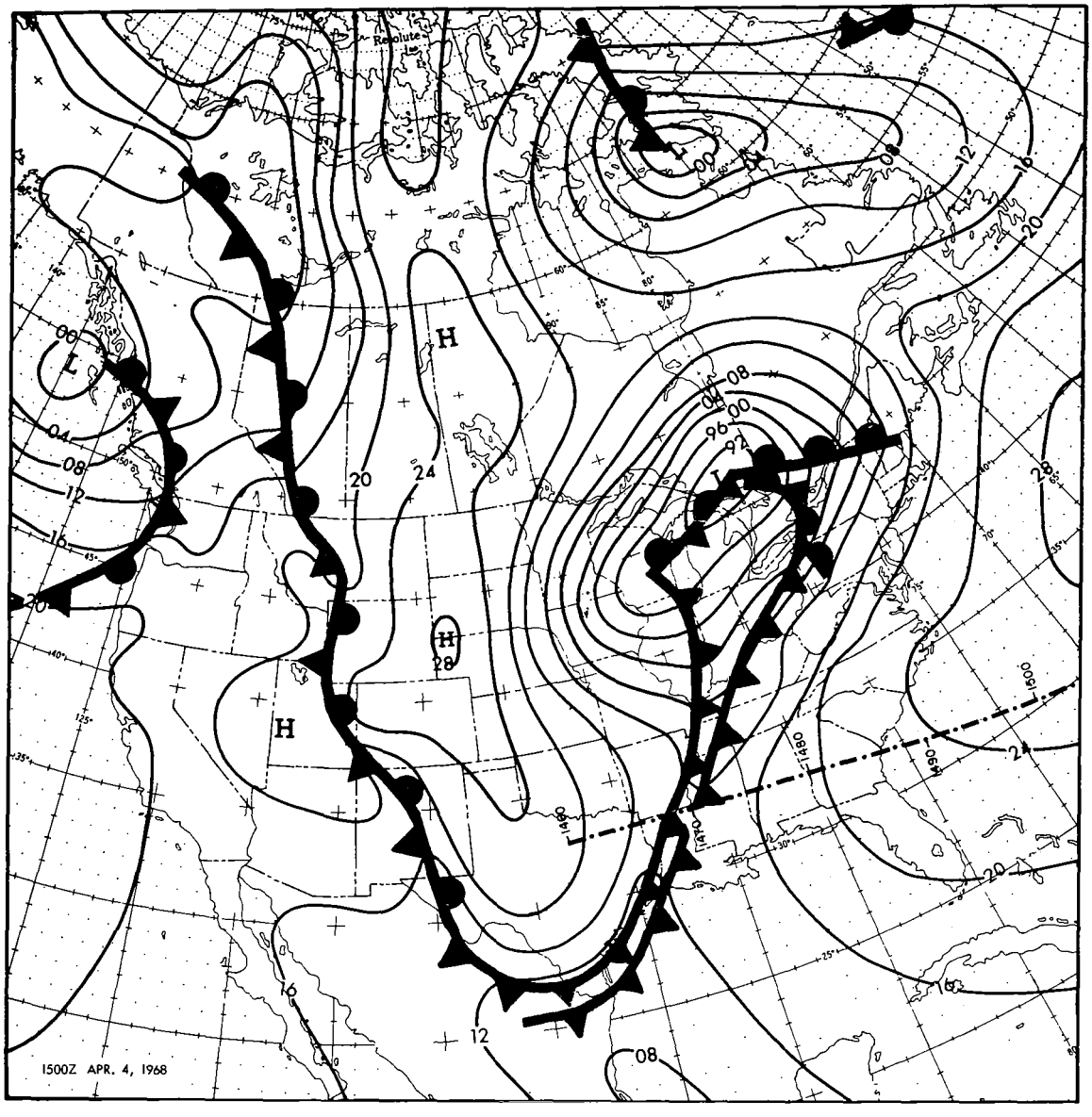

Figure 8—NMC surface analysis for 1500 GMT, April 4, 1968. The dot-dash line indicates the Apollo 6 subsatellite track, with the Apollo frame numbers shown along the track.

4. QUALITATIVE COMPARISON BETWEEN AN APOLLO 6 FRAME AND CONCURRENT ATS 3 DATA

Figure 9 gives an example of the comparison of an Apollo 6 frame with the concurrent ATS 3 4X and 1X photography covering the same area. Apollo 6 frame 873 was taken at 1346 GMT, while the ATS 3 measurements were acquired about 1 minute earlier. Therefore, a precise cloud-to-cloud comparison can be made of the common cloud field sensed by the cameras on the two spacecraft. The Apollo 6 photograph reveals a variety of cloud types and sizes from small cumulus clouds to

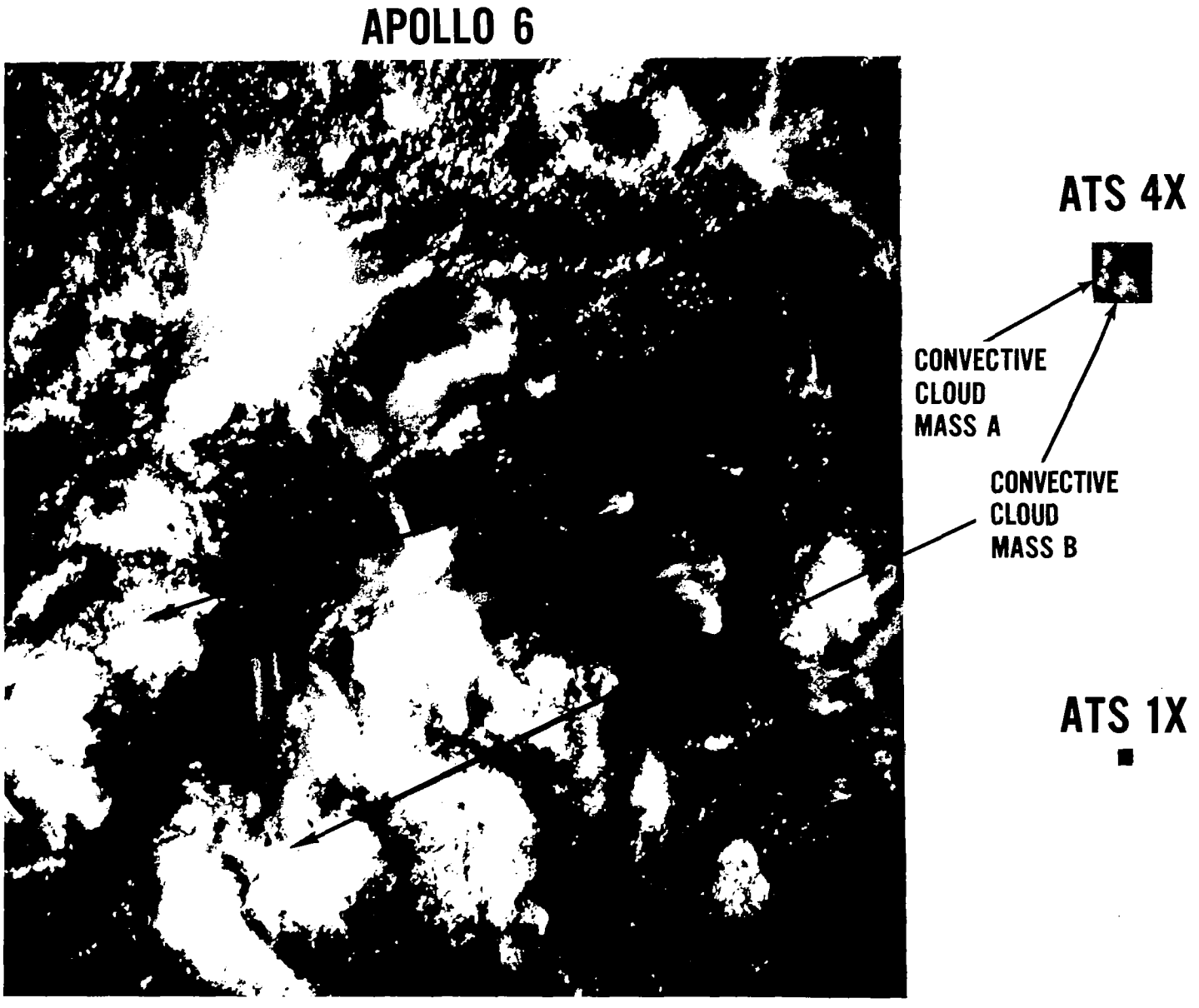

Figure 9—The comparison of Apollo 6 and ATS 3 photography over the Atlantic Ocean, where the area covered by each of the three photographs is approximately the same.

cumuliform clouds several km in size with cirrus blow-off apparently from their tops. Cumulus cloud streets, observed in the northwest corner of the picture, are associated with more organized activity connected with the weak stationary front noted in Figure 2. The cloudiness in the southeast corner of Figure 9 lacks the same degree of organization and is probably caused by local circulations.

The Apollo 6 prints used in the analysis, like the one shown in Figure 9, were square pictures, about 20 cm on a side. For an eye with resolving capability of 1 arc-minute and with the picture 25 cm from the eye, an analyst could detect clouds 60 m across (based on 140 X 140 km earth coverage). This is a factor of 2 less than in the indicated resolution capability of the emulsion. The same area covered in the Apollo 6 frame 873 appeared in the ATS 3 4X and 1X prints as areas 1.25 and 0.3 cm on a side, respectively, in the 8 X 10 prints used in the analysis. With the same assumptions regarding the observing distance from the print and the resolving power of the eye, cloud sizes of 0.8 and 3.4 km would be detected. Both of these figures are better than the spatial resolution of the ATS 3 spin-scan camera; therefore, the eye could detect the full resolving capability of the satellite sensor. The resolution of the spin-scan camera was not 3.7 km at the location of Apollo frame 873 because this frame was some 44 deg of great-circle arc removed from the ATS 3 subsatellite position (0°, 84° W). Whereas the eye could detect the maximum sensor resolution of the ATS 3 MSSCC in the 1X prints, these prints do not appear to contain the same resolution that is present in the 4X prints. A magnifying glass was used to enlarge Area *A* in the 1X print (Figure 2) to be comparable in size with Area *A* in the 4X print (Figure 3), but the latter still indicated more detail in the cloud patterns than the 1X print. Thus, it was concluded that the resolution in the 1X print was affected by the photographic process used to prepare the print. The ATS 1X prints appeared to have a spatial-resolution degradation of about 1.5 to 2 from the 4X prints. This subjective estimate was based on the relative appearance of the cloud patterns.

The effects of the lower sensor resolution of the ATS 3 data are clearly seen in Figure 9. Although some detail is lost through photographic reproduction from the original prints, the ATS 3 sensor resolution precludes the resolvement of the individual cloud elements in the cumulus cloud field shown in the top center of the Apollo photograph. The spacing between most of the elements is less than the resolution of the ATS 3 sensor even at the subsatellite point. As a result, the appearance of this type of cloud field in the ATS 3 4X photograph is a grey level which is brighter than the grey level that represents clear skies over the ocean (and shows the relatively low reflectance of the ocean in this portion of the visible spectrum). The grey level in the 1X photograph for this region is more difficult to assess but appears to be similar. In the 4X print the grey level is not as bright as it would be when the sensor field of view is filled with cumuliform clouds, but this condition could indicate a completely filled field of view for cirriform clouds. An example of cloud-filled resolution elements is shown slightly below the center of the picture where substantial cumuliform cloud masses were present. The one closest to the center of the picture was about 20 km across. This cloud mass appears clearly in the 4X picture at the northern end of the merged cloud mass slightly below center in the photograph. A small increase in the brightness there is associated with this strong cumulus development.

There is no evidence of a cloud type difference between the apparent cirrus blow-off from the convective towers and the towers themselves in the ATS 3 prints, whereas the cloud types are clearly discernible in the Apollo 6 picture. Also, it is not possible to detect multiple-level cloudiness in the ATS 3 photographs. However, when a sequence of ATS 3 pictures was viewed in time lapse, the

differential motion of the separate levels did permit the determination of multiple layers (Blackmer et al., 1970).

The break between the convective cloud masses *A* and *B* is easily seen in the ATS 3 4X print. There is a patch of cirrus between the two masses which is visible in both the Apollo 6 picture and in the 4X print (but not identifiable as cirrus in the latter). The nearly clear areas in the Apollo print, between the sections of cloud mass *B*, are seen as slightly dimmer regions in the ATS 3 4X picture and are not detectable in the 1X picture.

The spatial resolution of the ATS 3 sensor was insufficient to resolve the individual cloud elements in the cumulus cloud fields and to indicate the relatively clear regions between large cloud masses. The percentage of cloud cover was overestimated in these areas because any brightness measurement above a specified threshold was considered to be a completely cloud-filled resolution element. The effects of resolution were also seen in the capability to identify cloud types. The cloud patterns and the varying amounts of brightness seen in the ATS 3 photograph within the Apollo 6 picture field of view provided some identification of cloud type but not the almost certain identification that was possible with the Apollo 6 photograph. Conover (1962, 1963) has provided a semi-quantitative method for cloud type identification via meteorological satellites based on cloud organization, brightness, and spacing. This identification method was developed using TIROS photography, but, as the ATS 3 and ESSA 3 spatial resolutions were not markedly different, the method was applied to the data from these spacecraft also. In the ATS 4X picture, within the area covered by Apollo 6 frame 873, the cloud types were judged to be a combination of cumulus congestus, small cumulonimbus, stratocumulus, and altocumulus. Argument can be made for the presence of all of these cloud types in the Apollo 6 photography shown in Figure 9, the dominant cloud types being cumulus congestus and small cumulonimbus. The Conover (1963) method gave no indication of the cirrus that were detached from the cumulonimbus cells nor of the presence of the small-scale cumulus clouds. The importance of the resolution was demonstrated again by the incapability of the ATS 3 sensor to resolve the cloud streets in the upper left-hand corner of Figure 9. Conover (1963) does indicate a cloud street category in his cloud type identification method but in this case the banded structure could not be resolved.

When the clouds seen in Apollo 6 frame 873 were viewed as a series of stereographic picture pairs, it was discovered that the cirrus that appeared to be blown from the tops of cumulonimbus clouds actually were separated vertically from the lower clouds. There were no cumulonimbus clouds present; the maximum cumulus development was cumulus congestus with some altocumulus spreading outward from the congestus. Some of the cirrus did appear to be the product of convective activity, but either the cirrus (which for a given cloud size have a longer lifetime than cumulus) were advected from another region or remained in the area after the cumulonimbus had dissipated. The stereographic viewing of frame 873 indicates that even with high-spatial-resolution imagery, errors can still be made in the judgment of cloud types. A combination of high-resolution infrared (to provide cloud-top height measurements) and visible measurements also would have given a three dimensional picture of the cloud structure. The infrared measurements should be made in an atmospheric window (one, for example, of 10 to 11 μm) and in spectral regions that are most opaque for cirrus clouds in order that accurate cloud height estimates could be made for all cloud types.

5. QUANTITATIVE CLOUD ANALYSES OF BOTH APOLLO 6 SEGMENTS

A quantitative analysis of the percentage of cloud cover recorded from each satellite was performed along the center line of the Apollo 6 photographs. The Apollo 6 center-line position was established on the pictures from the other satellites by matching the positions of individual cloud masses identifiable on the pictures from each spacecraft. Cloud cover percentages from the Apollo pictures were estimated by one analyst, whereas two analysts determined the percentages from the ATS 3 and ESSA 3 photographs. In addition, the cloud types were determined for the data from the three satellites: for the Apollo 6 photographs, through the use of recognition by one analyst; for the ATS 3 and ESSA 3 pictures, with Conover's method by the same analyst, analyst 1, and with experience by another analyst, analyst 2, knowledgeable in the interpretation of satellite photography.

An example of the cloud information extracted from the photographs is shown in Figure 10. This portion of Apollo segment 1 shows information for the percentage of cloud cover and cloud type along the center line from the midpoint of Apollo 6 frame 906 to the midpoint of frame 912. Only the Apollo 6 center-line data and the ATS 3 4X data (for the two analysts) are shown; the cloud information for the ESSA 3 data and the remainder of the ATS 3 data were displayed in a similar fashion. The dark areas along each line in Figure 10 represent regions where clouds were judged to be present. The cloud cover symbols for analyst 1 are those given by the Conover method for each cloud category, whereas the symbols for analyst 2 were based on his experience.

The spatial resolution of the ATS 3 and ESSA 3 sensors was such that overestimates of the percentage of cloud cover were expected. Therefore, attempts were made to correct for the resolution effect. The first analyst specified the Conover-method cloud cover symbols, scattered, broken, and overcast, to indicate roughly the percentage of cloud cover over the entire region dominated by a particular cloud pattern and brightness level. The symbols were applied only to the portion of each region that appeared to be completely cloud covered. The weights given to the symbols used in Figure 10 and in other figures in this report are given below:

Symbol	Value (%)
⊖	30
⊖ – ◍	50
◍	80
◍ – ⊕	90
⊕	100

The tick marks, indicating the midpoint of each even-numbered Apollo 6 frame, are shown in Figure 10 for the corresponding positions on the ATS 3 4X pictures. The distance between midpoints shown

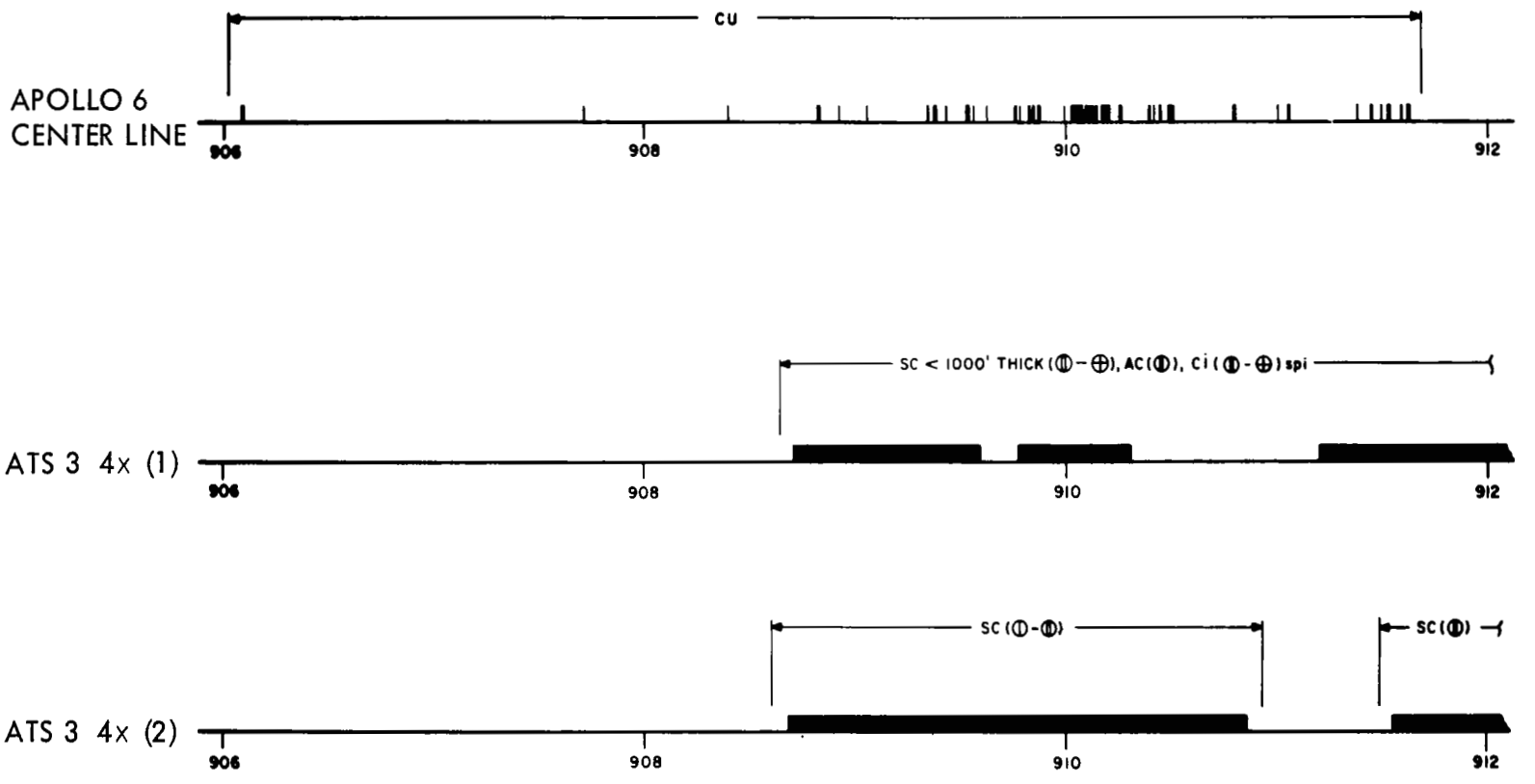

Figure 10—The cloud type and cloud cover information along the center line of the Apollo pictures, and the concurrent lines from the ATS 3 4X photographs, from the midpoint of Apollo 6 frame 906 to the midpoint of frame 912. The second and third cloud lines are for analysts 1 and 2, respectively, for the 4X photographs. Dark areas are shown to indicate completely cloudy regions.

in the figure is close to that of the Apollo pictures, but, for the ATS 3 and ESSA 3 pictures, this distance was considerably less. Thus, the data for these two satellites had to be stretched substantially to fit the scale of the Apollo cloud line. This stretching was particulary severe for the ATS 3 1X pictures, which were expanded by about two orders of magnitude. As a result, the alignment of the Apollo 6, ATS 3, and ESSA 3 cloud positions was not always perfect. Offsets of 15 km in cloud positions along the center line were possible, especially for the ATS 3 1X positions. For this reason, comparisons of cloud type and cloud cover for small areas along the Apollo center line were made cautiously. Generally, sections of cloud lines 150 km long or greater had to be used before meaningful conclusions could be drawn (unless the relative position of the cloud lines was established with greater precision than was usually the case). The relative positions were the most accurate for the ATS 3 4X data from Apollo segment 2 and from the western half of segment 1. This was because the viewing was less oblique, which allowed for less stretching of the data. For the ESSA 3 pictures, the viewing perspective was best at the extreme eastern end of segment 1. The possible effects of errors in relative cloud location on the estimate of the percentage of cloud cover for the Apollo data were examined by obtaining the cloud cover information from the Apollo pictures along lines approximately 15 km to either side of the center line. On some photographs the difference in the cloud cover from along one of the outer lines to along the center line was 10 to 15 percent, whereas the difference over larger areas was generally considerably smaller.

In Figure 10, the cloud type in the Apollo pictures was considered to be cumulus for the approximately 400-km portion of segment 1. Estimates of cloud type by the two analysts (the first using the Conover method, the second his experience) for the ATS 3 4X pictures showed that both analysts included stratocumulus. Use of the Conover method also indicated the possibility of some altocumulus and cirrus. Both analysts overestimated the percentage of cloud cover even when the apparent cloudy areas were weighted by the percentages associated with the cloud cover symbols. The overestimation was substantial due to the spatial resolution and the viewing perspective. ATS 3 was located at a local zenith angle of about 65 deg for the region where Apollo 6 frames 906 to 912 were taken (Figure 1).

A simple cloud model was developed to correct for the oblique views of clouds as seen from ATS 3 and ESSA 3. The effect of the view on accurate estimates of true cloud cover is largely dependent on the cloud size, spacing, and type distributions. Oblique views of clouds that are spaced far apart and have large thickness to width (T/W) ratios will result in the most serious overestimates of the true percentage of cloud cover. The other extreme is a large thin cloud mass with a small T/W ratio.

No attempt was made to compute T/W ratios for the individual cloud elements seen along the center lines of each Apollo photograph. This can be done by a stereographic technique described by Whitehead et al. (1969). However, due to the large amount of data involved, the technique was considered impractical for this investigation.

Figure 11 depicts a schematic vertical cross section showing the amount of the earth covered by a rectangular cloud (T/W = 0.5) and a square cloud (T/W = 1.0) viewed at local zenith angles of 20 and 50 deg. This model assumes that there is sufficient spacing between the clouds such that there is no possible overlap in the earth coverage caused by an adjacent cloud and that the sides of clouds rise vertically from their bases. For a cloud with T/W = 1.0 viewed at a local zenith angle of 20 deg, the

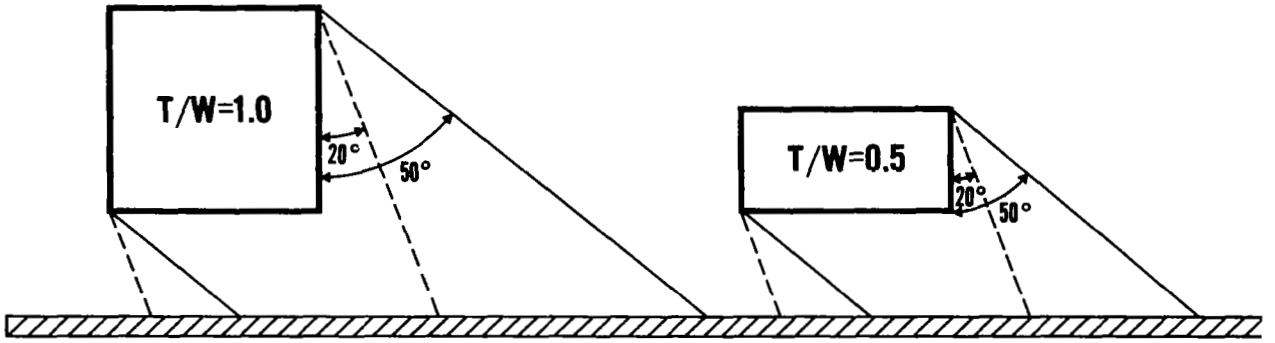

Figure 11—The effects of perspective illustrated by a vertical cross section of a square cloud (T/W = 1.0) on the left and a rectangular cloud (T/W = 0.5) on the right. Viewing angles of 20 and 50 deg are shown. The distance between the two ground intercepts for each of the angles determines the amount of the surface that is obscured by the cloud at that angle.

increased earth cover would be 1.3 times the width of the cloud. This perspective weighting correction decreases to 1.18 for a cloud viewed at the same local zenith angle where T/W = 0.5. Table 2 lists the perspective weighting corrections for local zenith angles between 20 and 75 deg. This table shows that these corrections are sizeable especially for local zenith angles greater than or equal to 60 deg.

Table 2—Perspective weighting corrections to be multiplied by the cloud cover viewed at a local zenith angle of 0 deg (rounded off to the nearest 0.05).

Cloud thickness to width ratio (T/W)	Local zenith angle						
	20°	30°	40°	50°	60°	70°	75°
0.5	1.20	1.30	1.45	1.60	1.85	2.25	2.90
1.0	1.30	1.50	1.80	2.20	2.75	3.85	4.75

A. Statistical Analysis of the Cloud Cover for Apollo Segment 1

Cloud information was extracted from the Apollo 6, ATS 3 4X and 1X, and ESSA 3 pictures for Apollo segment 1 and placed on worksheets similar to the one shown in Figure 10. The cloud comparisons were made only between Apollo 6 pictures and ESSA 3 4X and 1X pictures eastward from Apollo frame 882; as seen from ESSA 3, the view west of that Apollo frame was too oblique to permit satisfactory identification of clouds common to the Apollo 6 and ESSA 3 data such that the Apollo center-line position could be confidently established on the ESSA 3 photograph (frame 5). Eastward from Apollo 6 frame 908, ESSA 3 frame 6 was analyzed to see if a different view of the same area revealed any startling differences in percentages of cloud cover or identification of cloud type for the area of coincidence between the two ESSA 3 photographs.

The percentage of cloud cover within Apollo segment 1 was computed by dividing the segment into 17 worksheets where the Apollo center-line length on each worksheet was nearly equal. Then, each worksheet was subdivided into 200 units of equal length. The number of cloud-filled units was tabulated for the Apollo 6, ATS 3, and ESSA 3 cloud lines on each worksheet. Division of this number of units by 200 produced the recorded percentage of cloud cover for each worksheet. The number of cloud-filled units was also tabulated for cloud lines about 15 km to either side of the center line on the Apollo 6 pictures. Then the weighting factors (from the Conover method and from analyst experience) were applied by the two analysts to the ATS 3 and ESSA 3 data for the cloud-filled regions along the cloud lines to produce an adjusted cloud cover percentage. A single decision regarding the weighting factor was made by the analyst using his satellite interpretation experience; this was not always the situation when the Conover method was applied. Occasionally, there were cloud patterns for which two or more cloud categories offered equally plausible possibilities. Also, it was not uncommon to have different weighting factors associated with one category. Therefore, a maximum and a minimum weighting factor was applied to regions where these situations occurred, and for each worksheet, a maximum and a minimum adjusted percentage of cloud cover were indicated.

Table 3 is an example of the tabulations that were made for each cloud line from the ATS 3 and ESSA 3 pictures that was compared with the Apollo 6 cloud line in Apollo segment 1. The decisions as to cloud type are not shown. This particular example is for analyst 1 who employed the Conover method with the ATS 3 4X measurements. The numbers at the bottom show the average percentages of cloud cover for the Apollo center line before and after the Conover adjustment factor was used. After the Conover weighting factors were applied, the resulting maximum and minimum possible cloud cover percentages were indicated and the difference was only 1.4 percent. Thus, the cloud type determination ambiguities did not lead to a large spread in the estimated cloud cover percentages.

Without the Conover cloud cover adjustment the measured percentage of cloud cover for the 4X data by analyst 1 was 58.5 as compared with 45.5 from the concurrent Apollo 6 center line. Cloud cover percentages of 44.3 and 48.8 were measured 15 km from the Apollo center line on the north and south sides, respectively, and the average of the three cloud lines was 46.2 percent. Thus, the measurement of the percentage of cloud cover along the Apollo center line was reasonably representative of the average cloud cover conditions within 15 km of the line. The Conover-adjusted average cloud amount reduced the ATS 3 4X measured cloud amount to 51.8 percent, still 6.3 percent higher than the Apollo center-line measurement. This difference possibly can be explained by the viewing perspective which will be quantitatively examined later.

Table 4 depicts the percentages of cloud cover from the ATS 3 4X and 1X pictures for both analysts. The adjusted percentages for the second analyst are listed in the column labeled maximum adjusted cloud cover. There was consistency in the percentages measured by the two analysts from the 4X photographs which was not as good from the 1X photographs; the difference primarily was due to disagreement in the regions where small cumuliform clouds were present. In these areas, the brightness levels indicated on the 1X photograph were just above or below the individually set (and therefore slightly different) cloud/no-cloud threshold established by each analyst. The 4X data analysis revealed no substantial disparity between analysts when the small cumuliform cloud regime was present.

Table 3—Recorded and adjusted percentages of cloud cover for analyst 1, Apollo segment, from the ATS 3 4X photography, and the concurrent percentages from the Apollo 6 photography.

Apollo 6 frames	Recorded ATS 3 cloud cover (%)	Adjusted ATS 3 cloud cover (%)	Apollo 6 cloud cover (%)
836-840	58.3	46.6	38.0
840-846	54.3	43.4	43.1
846-852	44.8	max 37.3 min 36.3	38.5
852-858	63.1	56.5	70.0
858-864	53.2	max 52.1 min 47.1	43.6
864-870	96.5	max 88.7 min 84.2	84.5
870-876	39.4	35.8	54.6
876-882	43.3	40.1	35.0
882-888	84.6	82.1	90.4
888-894	99.3	98.2	100.0
894-900	56.9	max 46.8 min 45.5	18.6
900-906	33.0	max 29.7 min 26.4	15.7
906-912	37.1	max 33.4 min 29.7	7.4
912-918	50.2	max 45.2 min 40.1	20.1
918-924	60.2	48.1	17.1
924-930	57.1	45.7	38.4
930-935	63.4	62.5	58.5
Averages	58.5	max 52.5 min 51.1	45.5

Table 4–Percentages of cloud cover from the ATS 3 and Apollo 6 data for Apollo segment 1. The numbers in parentheses indicate either analyst 1 or 2. The maximum and minimum adjusted percentages are the result of ambiguities in the determination of cloud type by analyst 1 using the Conover method.

Photography	Recorded cloud cover (%)	Maximum adjusted cloud cover (%)	Minimum adjusted cloud cover (%)
Apollo 6	45.5	–	–
ATS 3 4X (1)	58.5	52.5	51.1
ATS 3 4X (2)	59.6	47.0	–
ATS 3 1X (1)	58.0	49.2	48.9
ATS 3 1X (2)	52.9	39.6	–

It is apparent from Table 4 that the Apollo cloud cover percentages are less than all the others except for the adjusted percentage determined from the 1X photographs by analyst 2. Thus, the overestimations noted for the 4X (1) photography are generally found for the rest of the ATS 3 data. There was little difference between the maximum and minimum possible percentages of cloud cover for the 4X and 1X pictures using the Conover method. The adjustment applied by analyst 2 resulted in greater differences between measured and adjusted cloud cover percentages than for analyst 1. This can be explained largely by the smaller weighting values (0.5 instead of 0.8) assigned to regions where low cloud types were identified.

Table 5 presents information similar to Table 4 for the comparison of the ESSA 3 data with the Apollo 6 photographs. Each ESSA 3 frame was considered separately. Frame 6 covers a portion of the region viewed by Frame 5, over an area of cirrus clouds, where the brightness levels in the eastern portion of the two frames appeared to be different. The digitized pictures over this eastern part of Apollo segment 1 were produced from a combination of the measurements contained within frames 5 and 6. Table 5 shows that no estimated percentage from the ESSA 3 data was as high as the corresponding Apollo 6 percentage, although it was expected that the results would be similar to those observed in Table 4 for the ATS 3 measurements. A plausible explanation for the difference is the degradation that the vidicon camera had experienced after the ESSA 3 launch, due to a colder than desired housing temperature. The loss of sensitivity was particularly dramatic just off the West Coast of Africa where an extensive region of cirrus associated with a jet stream was located. Apollo 6 frame 931 (Figure 12) indicates the nature of this cirrus, which was dense over portions of the picture. This same region is seen just west of Africa at 18° N, 18° W in the best ESSA 3 photograph of the area (Figure 4). Some evidence of the cirrus clouds was present, but the coverage and expected brightness were not commensurate with what was expected after viewing Apollo 6 frame 931. A substantial underestimation of cloud cover was made in this region and contributed to the general cloud cover underestimates that were made for the entire area viewed by ESSA 3. After the adjusted factors were applied, the estimate was low by almost a factor of 2 as figured by analyst 1 for frame 6.

Table 5—Percentages of cloud cover for concurrent areas from the ESSA 3 and Apollo 6 data for Apollo segment 1. The numbers in parentheses indicate either analyst 1 or 2. The maximum and minimum adjusted percentages are the result of ambiguities in the determination of cloud type by analyst 1 using the Conover method.

Photography	Recorded cloud cover (%)	Maximum adjusted cloud cover (%)	Minimum adjusted cloud cover (%)
Apollo 6*	40.7	–	–
ESSA 3 frame 5 (1)	40.6	34.5	34.2
ESSA 3 frame 5 (2)	32.7	25.8	–
Apollo 6*	31.3	–	–
ESSA 3 frame 6 (1)	23.0	16.3	–
ESSA 3 frame 6 (2)	24.5	20.5	–
ESSA 3 digitized (1)	39.9	–	–
ESSA 3 digitized (2)	34.4	–	–

*Corresponds to the ESSA 3 frame immediately following.

A method to objectively determine the percentage of cloud cover from the ESSA data has been developed by Miller et al. (1970). The percentage is estimated from the reflected energy received by the satellite: the higher the reflectance, the greater the percentage. Figure 13 depicts the superposition of the center line of Apollo segment 1 on isopleths of cloud cover (in eighths) for the concurrent ESSA 3 data from the Miller method. A cover of 1 to 2 eighths is indicated in the area of Apollo 6 frame 931 where extensive cirrus was located. This estimate is much too low compared with the average for Apollo frames 930 and 932 which was computed to be about 60 percent. Between Apollo 6 frames 902 and 914 the Miller method shows a cloud-free region along the Apollo 6 center line. The Apollo percentages of cloud cover in the region ranged between 1.2 (frame 908) and 18.4 (frame 910) with an average of 11 between these extremes. Thus, the cumuliform clouds that were present were undetected by the Miller technique when applied to the ESSA 3 measurements.

Figure 14 contains Apollo frame 890 and shows a cirrostratus overcast that becomes less dense in the right-hand half of the picture. The Miller technique indicates a cloud cover gradient across this picture from 7 eighths under the western portion to 3 to 4 eighths over the eastern portion (Figure 12). It is apparent that the reflectivity gradients noticeable in an overcast cirriform cloud cover can lead to substantial differences in cloud cover estimates when the same brightness criteria are applied to all cloud types. These criteria, therefore, must be set differently for cirriform clouds. Detection of cirrus clouds is important when brightness measurements are used to estimate the cloud cover. Miller has evaluated his method with and without the presence of cirrus clouds; the cloud cover brightness relationships are the most accurate when cirrus are not present.

Figure 12—Apollo 6 frame 931, taken about 300 km west of the West African Coast, illustrating cirrus associated with a subtropical jet stream.

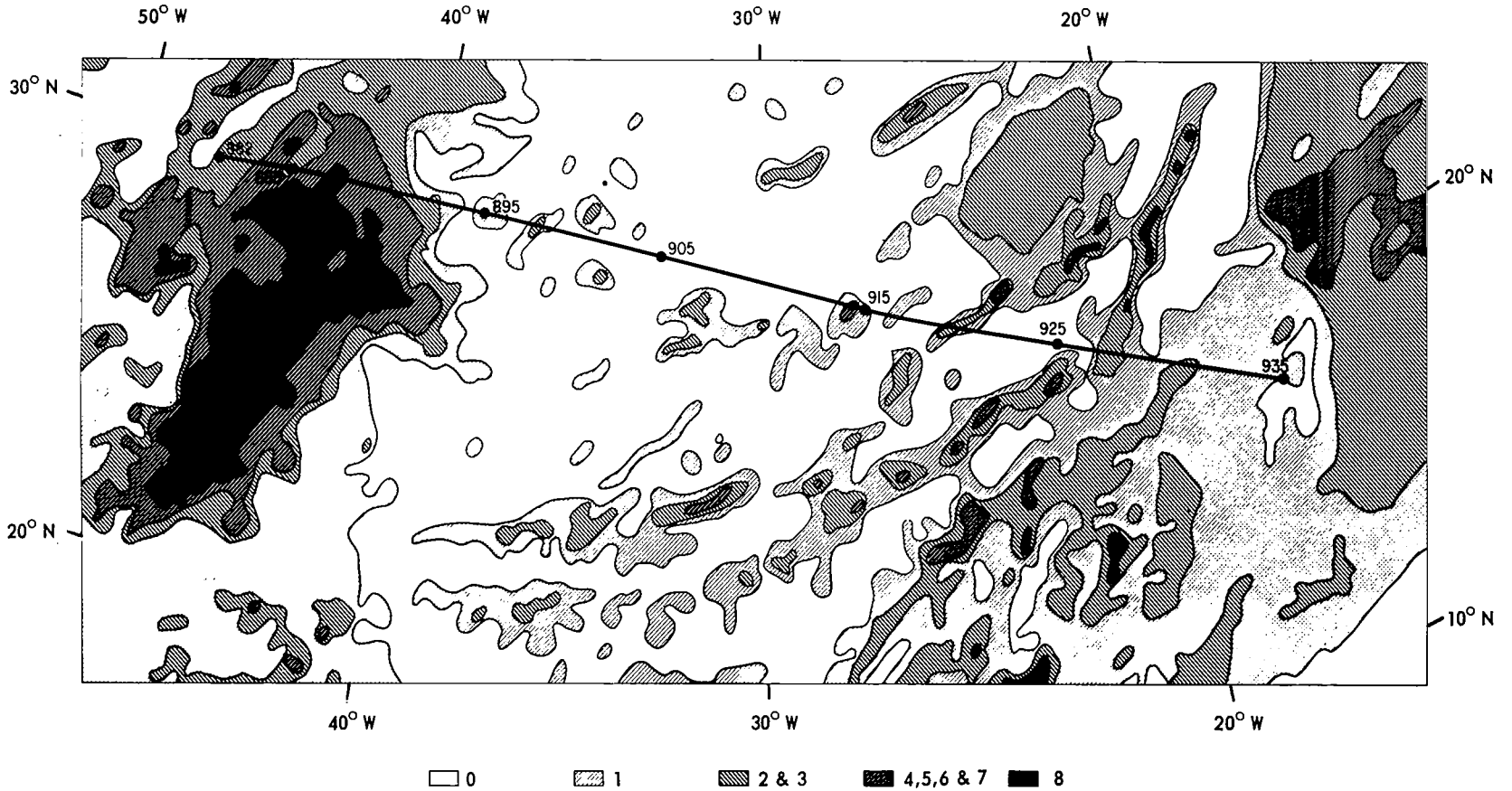

Figure 13–Cloud cover (in eighths) in the region traversed by Apollo 6 computed with the Miller et al. (1970) brightness method. The center line of the Apollo 6 track is indicated by the heavy solid line and selected principal point positions of approximately every tenth frame is indicated.

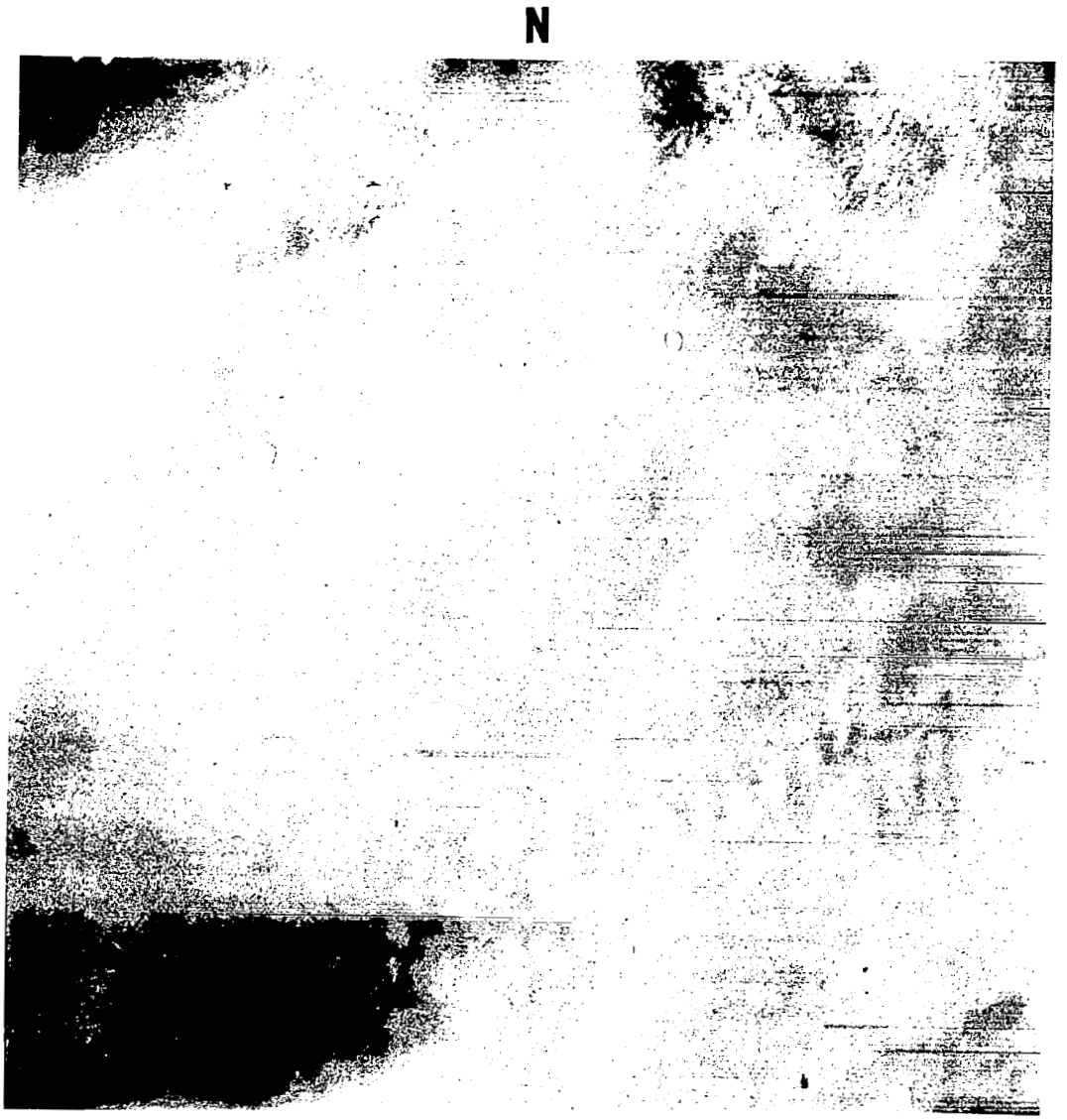

Figure 14—Apollo frame 890 showing cirrostratus that is less dense in the right-hand portion of the picture than in the left-hand portion.

The percentage of cloud cover using the Miller method for the ESSA 3 data covering Apollo segment 1, from Apollo 6 frame 882 to 935, was 18.4 versus 40.7 from the Apollo 6 calculation. Most of the difference probably resulted from the errors made in the three situations mentioned above (i.e., cirrus, cirrus reflectivity gradients, and small scattered cumulus).

Differences in results between the Miller method and the Apollo 6 pictures and between the Apollo 6 pictures and the ESSA 3 photographs were due most likely to the degraded state of the ESSA 3 sensor and were not necessarily produced by the methods used to estimate the percentage of cloud cover. However, it seems reasonable that the problems encountered with cirrus clouds by the Miller method would have occurred even if the sensor had suffered no degradation. These Apollo/ESSA comparisons emphasize that sensor degradations can substantially affect determina-

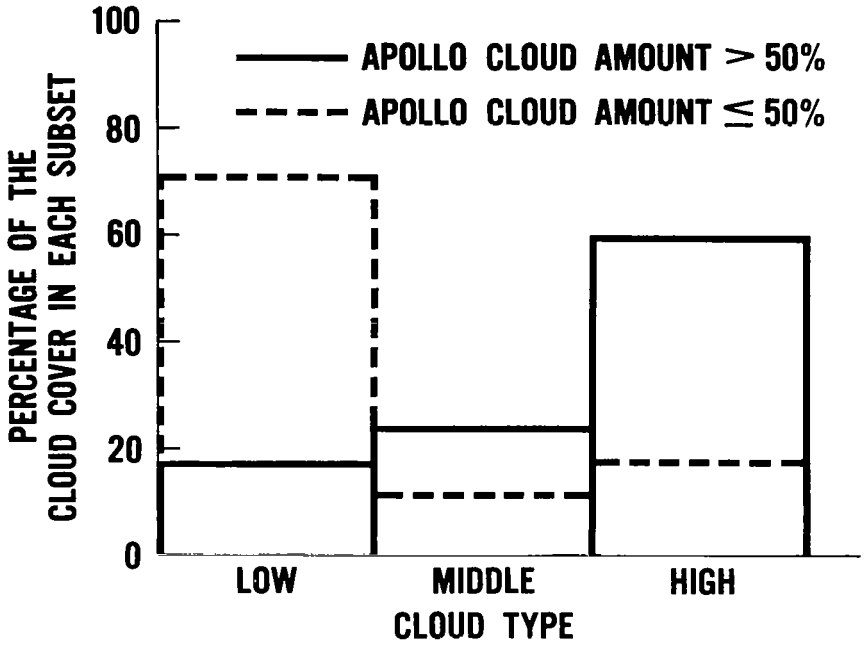

Figure 15—Histograms of the general cloud types (low, middle, and high) determined from the Apollo 6 pictures associated with each of the two data subsets within Apollo segment 1.

tions of the percentage of cloud cover. Therefore, these data must be either discarded or normalized to correct for the degradation. Normalization would not be possible in those regions where no clouds were detected.

Within Apollo segment 1 there appeared to be two basic cloud regimes. One was extensive cloudiness associated with organized systems of larger than mesoscale size, and the other was primarily cellular cloud patterns that were connected with weaker or local circulations. It was hypothesized that the greatest errors in estimating the percentage of cloud cover would occur within the areas where this latter cloud regime occurred. To test this hypothesis, Apollo segment 1 was divided into two subsets of data, the first where the Apollo percentage of cloud cover on a worksheet was less than or equal to 50 (approximately a 400-km cloud line) and the second where the worksheet percentage was greater than 50. Figure 15 indicates the cloud type distributions determined from the Apollo 6 data associated with each subset. The first subset had a very high percentage of low cloud types, which were most likely convectively produced with little middle and high cloudiness, whereas the second subset contained mostly clouds typical of organized systems, i.e., middle and high clouds.

The results of the subdivision for the ATS 3 measurements are presented in Table 6. Where generally large cloud masses were present (i.e., Apollo worksheet percentages greater than 50), the ATS 3 estimates of percentage were within ±4 of the Apollo 6 estimates. This was not surprising since the expected effects of perspective and sensor resolution are small with large cloud masses. However, when the Apollo percentage of cloud cover was less than or equal to 50, large overestimates,

by almost a factor of 2, occurred with the ATS 3 4X photographs. Some areas of scattered convective clouds went undetected in the ATS 3 1X pictures which affected the results of both analysts.

Table 7 indicates the percentage of cloud cover for the two subsets resulting from multiplication of the adjustment factors by the measured percentages of cloud cover. All the resulting percentages for the greater-than-50 subset are smaller than the Apollo 6 cloud cover by as much as 17 percent. However, there was only about 6 percent difference between the Apollo 6 percentage and the Conover-method adjusted results (analyst 1). Conversely, overestimates still occurred when the Apollo 6 percentages were less than or equal to 50, especially for ATS 3 4X pictures. In the case of 1X photographs, the estimated percentages were closer to the Apollo 6 results, due in part to areas of scattered cumulus going undetected in the photographs. Also, analyst 2 had smaller weighting factors than analyst 1 in these predominantly convective cloud regimes.

Table 6—Recorded percentages of cloud cover from the ATS 3 and Apollo 6 data for the two subsets of Apollo segment 1. The numbers in parentheses indicate either analyst 1 or 2. The maximum cloud covers are shown for analyst 1.

Apollo 1 segment 1 subsets	Apollo 6 cloud cover (%)	ATS 3 cloud cover (%)			
		4X (1)	4X (2)	1X (1)	1X (2)
Cloud cover >50%	76.3	74.4	72.4	80.0	77.3
Cloud cover ⩽50%	28.6	50.3	52.6	45.9	39.7

Table 7—Adjusted percentages of cloud cover from the ATS 3 and Apollo 6 data for the two subsets of Apollo segment 1. The numbers in parentheses indicate either analyst 1 or 2. The maximum cloud covers are shown for analyst 1.

Apollo segment 1 subsets	Apollo 6 cloud cover (%)	ATS 3 cloud cover (%)			
		4X (1)	4X (2)	1X (1)	1X (2)
Cloud cover >50%	76.3	70.0	59.3	71.1	63.3
Cloud cover ⩽50%	28.6	42.6	40.4	37.3	26.5

Perspective corrections were multiplied by the recorded Apollo cloud cover percentages for cloud sizes less than or equal to 7 km and less than or equal to 11 km as indicated along the center line (though the actual cloud sizes could be larger). For these clouds a T/W ratio of 0.5 was used. This seemed to be a reasonable compromise between clouds with a greater ratio, such as cumuliform, and clouds with a smaller ratio, such as cirrus. (It was assumed that for clouds larger than 11 km the average T/W ratio would be small, and the perspective correction would be nearly negligible. Therefore, these clouds were not considered for this calculation.) The total cloudiness for a worksheet was not permitted to rise above 100 percent. The perspective weighting corrections were probably quite conservative given the assumptions of vertical cloud walls and large spacing between clouds. The perspective corrections from Table 2 were applied along with the viewing perspective information for the ATS 3 data from Figure 1.

When the corrections were applied, the percentages of cloud cover increased to 53.2 and 54.9 for the groups with a 7-km and an 11-km size maximum, respectively. Thus, the application of the perspective correction to cloud sizes between 7 and 11 km did not increase the percentage of cloud cover substantially. This indicates that the 7-km upper limit on cloud size is a reasonable selection for purposes of perspective correction in Apollo segment 1.

Most of the increase in cloud cover results came from the eastern end of the segment, where a combination of small clouds and large local zenith angles were present. The 53.2-percent cloud cover agrees closely with the ATS 3 4X (1) estimate obtained after adjustment with the Conover method and is about 6 percent higher than that obtained by the second analyst through adjustment based on his experience.

Similar results were observed for the cloud cover less than or equal to 50 percent subset of Apollo segment 1 after the perspective corrections were made. This was the portion of the segment where smaller clouds predominated, and, therefore, the perspective corrections produced a sizeable increase from 29 to 40 (for the cloud sizes less than or equal to 7 km) in the estimated percentage of cloud cover. The corrected cloud cover percentage compares very favorably with the 42.6 and 40.4 adjusted percentages determined from the 4X pictures for analysts 1 and 2, respectively.

Perspective corrections were also applied to the Apollo data (frames 882 to 935) that were compared to ESSA 3 frame 5. The necessary viewing angles were determined with knowledge of the ESSA subsatellite point and the position of each Apollo frame when frame 5 was taken. As before, the 7-km and 11-km cloud size thresholds were used in this analysis. The resulting difference between the percentages for the two thresholds was again small (1.4 percent). For the 7-km maximum the corrected percentage of cloud cover was 45.5 as compared with 40.7 before the correction was made. When applied to the Apollo data, the correction widened the gap between the Apollo and ESSA percentages (Table 5).

B. Statistical Analysis of the Cloud Cover for Apollo Segment 2

The statistical analysis of the cloud cover for Apollo segment 2 was conducted in the same manner as the analysis of segment 1, with one minor exception. Due to greater variation in the distance between the midpoints of even-numbered pictures, the number of units could not be held constant for a given worksheet. This variability was largely a product of a spacecraft maneuver that began

around frame 1478. The distance between the midpoints of frames 1470 and 1472 was arbitrarily selected as 100 units; therefore, a variable number of units resulted for other pairs. Because the data were normalized to percentages of cloud cover, the slight differences in the methods employed for the analysis of each segment did not affect the interpretation of comparisons between the results of the two.

The total percentages of cloud cover from the ATS 3 and Apollo 6 data are given in Table 8. The Apollo 6 percentages at approximately 15 km north and south of the center line were 51.1 and 45.0, respectively. Thus, if the cloud location error for the ATS 3 data was always 15 km north of the center line, the percentage that would be compared with the data would be about 6 percent higher. However, it is probable that the actual value that should be used for comparison would be only slightly higher than the center-line value shown in Table 8.* The results from Table 7 are almost the same as those from Table 4 for segment 1. Sizeable overestimates in the percentages again were made using the ATS 3 data, and these overestimates were slightly larger than those found in segment 1. This is somewhat surprising since the perspective view of the clouds from ATS 3 was less oblique for segment 2. Once again, the differences between maximum and minimum percentages of cloud cover were small when the Conover method was employed by analyst 1. The results of the two analysts agreed very well for the recorded cloud cover from the ATS 3 4X pictures and almost as well for the 1X pictures. An important difference between Tables 4 and 8 is that the measured percentages remained nearly the same for the 4X and 1X pictures in Table 8, while in Table 4 the 1X pictures for analyst 2 yielded smaller values. A possible explanation for the difference is that there were no sizeable areas in segment 2 where the cloud cover was small, as there were in segment 1 (especially between frames 900 and 925). As a result, the two analysts were rarely faced with difficult cloud/no-cloud threshold decisions in segment 2 when the 1X data were examined. At what point insufficient sensitivity and/or spatial resolution can lead to significant information loss is still unclear. In view of the difference in the results from each Apollo segment, it is likely that this occurs at or not far from the values of the spatial resolution and/or sensitivity associated with the 1X photographic presentation.

Table 8–Percentages of cloud cover from the ATS 3 and Apollo 6 data for Apollo segment 2. The numbers in parentheses indicate either analyst 1 or 2. The maximum and minimum adjusted percentages are the result of ambiguities in the determination of cloud type by analyst 1 using the Conover method.

Photography	Recorded cloud cover (%)	Maximum adjusted cloud cover (%)	Minimum adjusted cloud cover (%)
Apollo 6	44.8	–	–
ATS 3 4X (1)	63.3	55.2	55.0
ATS 3 4X (2)	64.7	53.1	–
ATS 3 1X (1)	62.1	55.3	54.6
ATS 3 1X (2)	66.1	51.9	–

*Since it is unlikely that the mislocation error was always 15 km north of the center line.

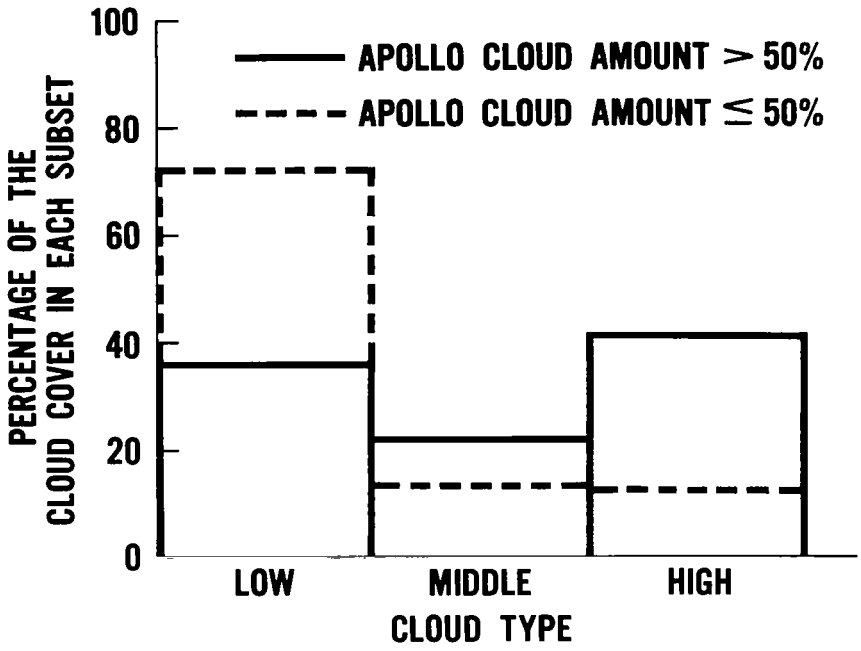

Figure 16—Histograms of the general cloud types (low, middle and high) determined from the Apollo 6 pictures associated with each of the two data subsets within Apollo segment 2.

Segment 2 was subdivided into two data subsets to study the percentages of cloud cover when two cloud regimes were present. The method for subdivision was the same as for segment 1. Figure 16 indicates the cloud type distributions for the two subsets. The distributions are similar to those obtained in segment 1, where the low clouds predominated for Apollo 6 percentages less than or equal to 50 along a 400-km line, and higher clouds predominated for percentages greater than 50. A comparison of Figures 15 and 16 reveals that with the Apollo percentage less than or equal to 50 there was a higher percentage of low clouds in segment 2 than in segment 1 (37 percent versus 16 percent).

Table 9 lists the recorded percentages of cloud cover from the ATS and Apollo measurements for the two subsets of segment 2 (Table 9 is similar to Table 6). For the 50-percent-maximum subset the results are nearly identical to the corresponding results from segment 1. However, the results for the other subset differ between segments 1 and 2. At least some of the difference may be due to the higher percentage of low cumuliform cloudiness present in segment 2 which was especially evident in Apollo frames 1506 to 1510. Each analyst made a substantial overestimate of the percentage of cloud cover for both the ATS 3 4X and 1X photographs for those frames. The indicated earth cover was nearly complete from all satellite data sources over the main portion of the frontal band (frames 1470 to 1475), and, therefore, the estimates of the percentage of cloud cover were close to or at 100. Frames 1476 to 1481 covered an area consisting primarily of broken middle clouds east of the most active region near the midlatitude front, and some overestimation occurred due to the ATS 3 spatial resolution not being sufficient to resolve the small openings in the cloud canopy.

Table 9–Recorded percentages of cloud cover from the ATS 3 and Apollo 6 data for the two subsets of Apollo segment 2. The numbers in parentheses indicate either analyst 1 or 2. The maximum cloud covers are shown for analyst 1.

Apollo segment 1 subsets	Apollo 6 cloud cover (%)	ATS 3 cloud cover (%)			
		4X (1)	4X (2)	1X (1)	1X (2)
Cloud cover >50%	82.2	97.7	96.2	98.4	100.0
Cloud cover ≤50%	20.5	40.9	44.1	38.5	44.9

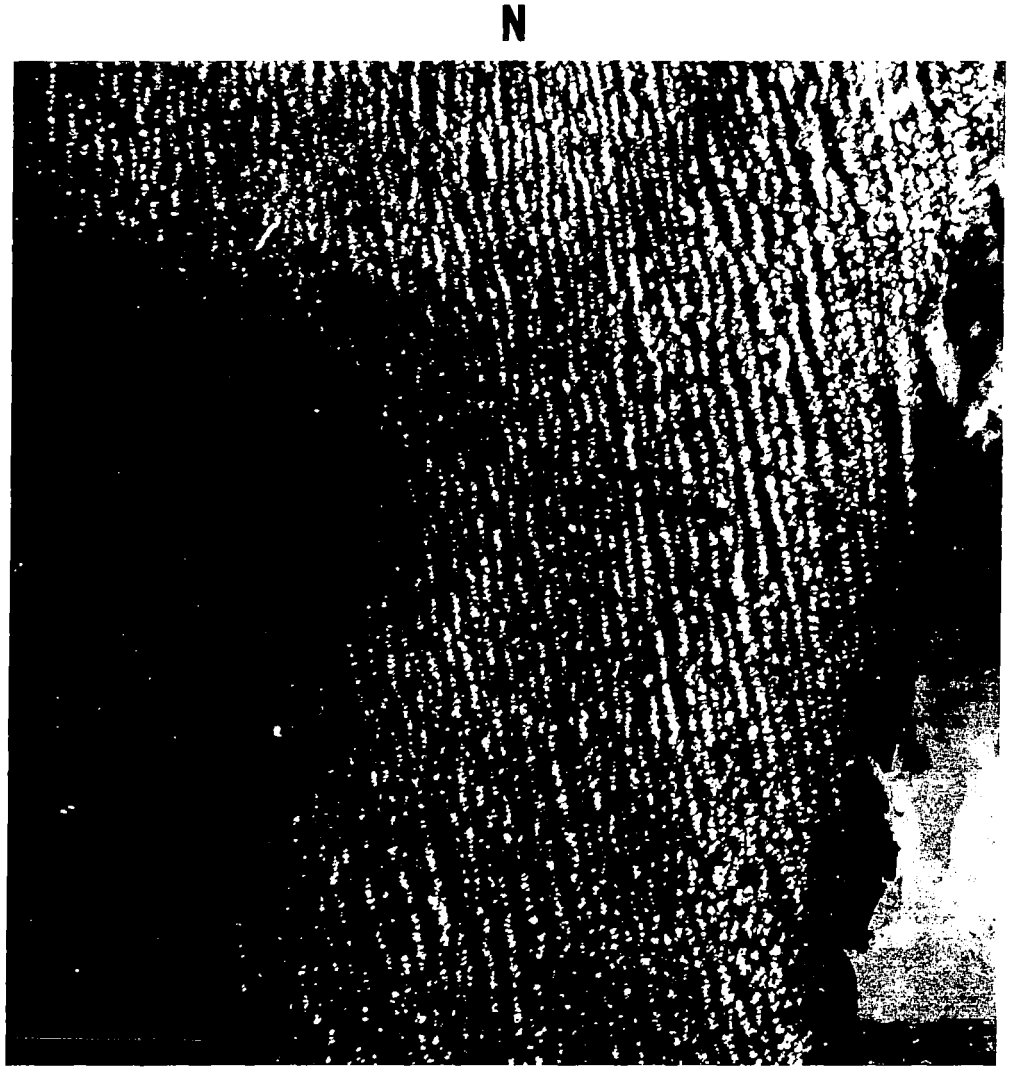

Figure 17–Cumulus cloud streets over Georgia (Apollo 6 frame 1484).

Table 10—Adjusted percentages of cloud cover from the ATS 3 and Apollo 6 data for the two subsets of Apollo segment 2. The numbers in parentheses indicate either analyst 1 or 2. The maximum cloud covers are shown for analyst 1.

Apollo segment 2 subsets	Apollo 6 cloud cover (%)	ATS 3 cloud cover (%)			
		4X (1)	4X (2)	1X (1)	1X (2)
Cloud cover >50%	82.2	87.6	79.0	88.4	80.2
Cloud cover ≤50%	20.5	34.1	36.2	33.8	33.5

Sizeable overestimation of the percentage of cloud cover occurred in the area covered by Apollo frames 1482 to 1487 in the Apollo cloud cover subset with a maximum of 50 percent. The Apollo cloud cover estimate was 14 percent, and the ATS 3 estimates ranged from 46 to 53 percent. Figure 17 contains frame 1484 which shows a series of cumulus cloud streets over southeastern Georgia. The average spacing of the cumulus streets was approximately 3 km, smaller than the subsatellite spatial resolution of the ATS 3 sensor. Along a given cloud street the spacing of individual cloud elements was even smaller; thus, the sensor could not resolve the individual elements. The estimate of the cloud cover over the cloud street region was 100 percent for the ATS 3 measurements whereas the true cloud cover was approximately 15 percent.

Application of the Conover-method and experience adjustments to each subset of segment 2 is shown in Table 10. For the second subset the adjusted cloud cover estimates are within a 3-percent range, for the ATS 3 pictures, unlike the results in Table 7 which had a range of 16 percent. All of the estimates for this subset are still considerably higher than the Apollo estimates. For the first subset in Table 10 the percentages for the 4X data are close to the Apollo percentage. This is in contrast to Table 7 for segment 1 in which the percentages adjusted by experience were considerably smaller than the Apollo amount. The higher concentration of cumuliform clouds in Apollo segment 2 for the first subset was probably the reason for this difference.

Perspective corrections were applied to segment 2 with the same cloud size thresholds that were employed in the analysis of segment 1. The clouds contained in segment 2 were viewed less obliquely than those in segment 1, and, therefore, the potential perspective effect was diminished. The calculated increase due to viewing perspective was 6½ percent (for cloud sizes less than or equal to 7 km) which was smaller than the 8 percent increase for segment 1. The resultant perspective-corrected percentage of cloud cover for segment 2 was 51.4. A further increase of 1.4 to 52.8 percent was noted when the perspective correction was used for the 11-km threshold. This result was similar to that for Apollo segment 1 and indicated that application of the perspective correction to the lower threshold was reasonable for segment 2 as well as for segment 1. Table 8 indicates that the perspective-corrected percentages were about 3 lower than the adjusted percentages for both the ATS 3 4X and 1X measurements [with the exception of the ATS 3 1X (2) results].

When the 50-percent-maximum subset was corrected for perspective viewing, the Apollo 6 result rose to 26 percent. This corrected figure was still some 8 to 10 percent lower than the adjusted figures for the ATS 3 data. Even with what was judged to be a conservative perspective correction and with an adjustment applied for the sensor spatial resolution the cloud cover was still overestimated by 3 to 10 percent in regions where the Apollo percentages of cloud cover were less than or equal to 50. It is concluded that the most probable cause of the discrepancy was insufficient adjustment for the sensor spatial resolution. This conclusion is not surprising in view of the results of Shenk and Salomonson (1971) who found that large overestimates of the percentage of cloud cover occurred unless the areal spatial-resolution element size was considerably smaller than the average areal cloud size. This is often not the case in subtropical and tropical areas having small convectively produced clouds.

Knowledge of the percentage of cloud cover has been important in the calculation of the albedo of the earth, which, along with measurements of the total emitted infrared energy, provides the data that are necessary to estimate the net outgoing flux at the top of the atmosphere. This flux measurement can be used to make estimates of the available potential energy being generated in the atmosphere.

Total earth albedo estimates have gradually decreased from 50 percent (Dines, 1917) to 30 percent (Raschke and Bandeen, 1970). The latter results come directly from data from a 0.2- to 4.0-μm channel on the Nimbus meteorological satellites that sensed a large majority of the energy reflected by the earth. The 30-percent albedo value was about 7 percent lower than the last previously accepted figures based on conventional data. If the percentage of cloud cover data that were being employed in the albedo estimate previous to the satellite measurements were overestimated, this would help explain the discrepancy between the conventional and satellite albedo determinations. The percentage of cloud cover overestimates that are shown in this study to result generally from satellite observations (and probably from conventional data as well) would indicate that satellite derived albedo measurements are more accurate than those made earlier from conventional data.

6. CLOUD TYPE DISTRIBUTIONS

Successful cloud type identification requires that there is sufficient information available such that the characteristics of a given cloud are distinguishable. Thus, information concerning cloud size, shape, spacing, texture, thickness, and height is useful for making a cloud type decision. When prints of the Apollo pictures were examined, the first four of these parameters were directly observable, and information on cloud height and thickness could be inferred. Data routinely received from meteorological satellites give less precise information on all of the parameters, especially texture. The comparison of the Apollo 6 and ATS 3 photographs made earlier (Figure 9) illustrated the lack of information on cloud texture in the 4X and 1X pictures. Improved information on cloud height and thickness is provided by stereographic viewing of Apollo picture pairs.

The high spatial resolution of the Apollo 6 photographs made it possible to examine the distribution of cloud types that are observed in the subtropics and tropics as well as that associated with the cold front over the lower Mississippi Valley. The first preparation of the distributions followed a simulation of the situation that would exist if the high-resolution data did not have the overlap necessary for stereographic analysis. After this, the original stereographic pairs were examined along

the entire length of both segments, and a comparison of the distributions from the two methods was made.

Table 11 presents the cloud type distributions for Apollo segment 1 derived without the benefit of stereographic viewing. The percentages listed are based on the areal coverage of each cloud type along the center line. There were numerous cases of multiple cloud layers where the cloud types could not be readily separated for a given region. These layered or merging cloud situations are shown where the principal cloud type is listed first and the complex cloud pattern is placed in the low, middle, or high cloud category based on the principal cloud type. Numerous multilayered conditions existed when middle clouds were the dominant cloud type and also were probably present with a solid cirrostratus overcast. The cloud type distributions indicate that the clouds tended to be either low or high. Some 65.0 percent of the total cloud cover consisted of clouds occurring at only one level. A few clouds of a different type were mixed in with the predominant type for another 5.3 percent of the distribution. Thus, about 70 percent of the total cloud regime was comprised essentially of a single level of clouds. All but 3.7 percent of the predominantly middle cloud coverage was in multilayered cloud situations. Therefore, the true percentage of middle cloud coverage is probably lower than the 19.0 percent indicated. A large percentage of the middle clouds were associated with the weakening frontal zone.

These general vertical cloud distributions indicate that cloud motions computed in the tropics from measurements received from geosynchronous satellites are applicable for clouds in the low levels (around 850 mb) or at high levels (around 200 mb). Often, differential cloud motions and the apparent lifetime of the cloud elements can provide the necessary information to distinguish between the high and low clouds as viewed from a geostationary satellite (Blackmer et al., 1970; Fujita, 1970).

Table 11—Apollo 6 cloud type distribution for Apollo segment 1, prepared without the assistance of stereographic viewing. The percentages are based on the portion of the total cloud cover assigned to each cloud type or combination of types.

Low Cloudiness		Middle Cloudiness		High Cloudiness	
Cloud type	Percentage of total cloud cover	Cloud type	Percentage of total cloud cover	Cloud type	Percentage of total cloud cover
Sc	23.8	Ac	1.3	Ci	23.1
Cu	13.4	Ac, Sc	0.5	Ci, few cu	2.4
Cu, Ci	1.3	Ac, Cu	7.4	Ci, Ac	2.1
Cu, few Ci	0.3	Ac, Cu (Sc)	5.5	Thin Ci	2.5
		Ac, few Cu, few Ci	1.2	Thin Ci, few Cu	0.7
		As	0.5	Cs	11.0
		As, Cu	0.4	Cb	0.4
		As, Cu (Sc)	1.5		
		As, few Cu, few Ac	0.7		
Total = 38.8%		Total = 19.0%		Total = 42.2%	

Table 12—Apollo 6 cloud type distribution for Apollo segment 2 prepared without the assistance of stereographic viewing. The percentages are based on the portion of the total cloud cover assigned to each cloud type or combination of types.

Low Cloudiness		Middle Cloudiness		High Cloudiness	
Cloud type	Percentage of total cloud cover	Cloud type	Percentage of total cloud cover	Cloud type	Percentage of total cloud cover
Sc	25.6	Ac	3.8	Ci	1.3
Cu	14.8	As	0.1	Thin Ci	0.4
Sc, Cu	6.3	Ac, Sc, Cu	1.9	Cs	17.7
		As, Ac	4.5	Cb	2.2
		As, Cu	4.4	Cs, As	2.5
		As, Sc	2.9	Cs, As, Cu	1.3
		As, Sc, Cu	2.3	Ci, Cu	1.0
				Ci, Sc	4.3
				Ci, Ac	0.3
				Ci, As	2.4
Total = 46.7%		Total = 19.9%		Total = 33.4%	

The most difficult judgment that it was necessary to make in determining the cloud type was to distinguish between altocumulus and altostratus. Also, it was not easy to distinguish between stratocumulus and altocumulus due to the similar appearance of the cloud tops for these two types. The scale of the cells in altocumulus was so small that there were times when they definitely gave the smoother appearance of altostratus. Therefore, the precision of the recorded percentages of altocumulus and altostratus is rather uncertain. Even higher spatial resolution than that of Apollo 6 photography may be necessary before a satisfactory judgment between these two cloud types can be made.

The distinction which the analyst made between cirrus and thin cirrus was based solely on an arbitrarily set brightness threshold. The subjective nature of the cirrus/thin cirrus threshold should be kept in the mind as one views Table 11 which shows that the percentage of the total cloud coverage attributed to thin cirrus or a combination of thin cirrus and cumulus was 3.2. If this percentage is divided by the percentage of cloud cover along the center line of Apollo segment 1, then the resulting earth coverage of thin cirrus is 1.4 percent. The earth coverage of cirrus, thin cirrus, cirrus with few cumulus, and thin cirrus with few cumulus was 13 percent. When cirrus and cirrus combinations with isolated low clouds occur and are not detected or identified, serious errors in the interpretation of infrared radiation measurements taken through an infrared-radiation window from above the cirrus level (e.g., meteorological satellite measurements) can result.

The cloud type distribution along the center line of segment 2 which was prepared without stereographic viewing is indicated in Table 12. This distribution had fewer high clouds, more low clouds, and about the same percentage of middle clouds as segment 1. As was the situation in segment 1, the middle clouds principally occurred in connection with activity near a frontal zone. It was

again difficult to distinguish between altocumulus and altostratus and between stratocumulus and altocumulus. In segment 2 the high clouds were nearly all associated with the strong cold front, whereas in segment 1, high clouds were present with a variety of meteorological conditions (i.e., a jet stream, a frontal zone, and tops of cumulonimbus). There were numerous cumulonimbus protrusions extending above the cirrostratus canopy associated with the front.

Because the Apollo 6 photographs were taken with approximately 55 percent of overlap between successive pictures, it was possible to examine stereographically the cloud information in the two segments. It was more difficult to view the latter portion of segment 2 (frames 1480 to 1510) stereographically due to the spacecraft's movement, which changed the viewing perspective slightly from frame to frame. The stereographic views permitted more positive cloud type identifications along the center line of each segment, and a comparison was made between the previous results and the cloud type determinations derived from examining the stereographic picture pairs. This comparison is of importance in assessing the effect of direct cloud height information on cloud type determination even when data are available with the spatial resolution of the Apollo 6 prints.

Most of the differences between the cloud type estimates made with and without stereographic viewing along segment 1 were minor. The stereographic views showed a number of areas where a cloud type had been identified improperly, especially isolated cirrus clouds which were incorrectly identified as middle clouds. However, there was one region where it was difficult to make a clear choice between a low and a middle cloud.

As analyzed without the stereographic viewing, stratocumulus was the dominant estimated cloud type from frame 836 to frame 856. This was in disagreement with the altocumulus cloud type estimates made in the same region by Kaltenbach.* A case could be made for either low altocumulus stratiformis or high stratocumulus stratiformis along this portion of the center line; both have a similar appearance (World Meteorological Organization, 1956), and both can have a layer of clouds below. This lower layer was clearly discernible in the stereographic views, but could not be determined decisively from the Apollo 6 prints alone. The height of the cloud tops of the upper layer (about 2 km) was calculated from the length of the cloud shadow on the ocean surface below with knowledge of the elevation angle of the sun. From near the center of frame 842 eastward through frame 856, the cloud type was relabeled as altocumulus rather than stratocumulus after viewing the stereographic picture pairs. This decision was based on the judgment that these clouds were at a slightly higher level and had a slightly smoother appearance than the stratocumulus to the west (frames 836 to 842). The layer below was judged to be small cumulus cells. The stereographic viewing not only showed the two distinct layers but also, by isolating the individual clouds, yielded a closer examination of the composition of each layer. The analysts tended to miss small details in cloud structure when examining prints in which all of the clouds appeared to be at the same level. This explains why some clouds were not easily placed into a cloud type category, even when the stereographic views were examined. The difficulty in the cloud type decision was attributable to cloud types that had the same appearance in the high-resolution photography and to cases where the cloud tops were at an altitude which could be associated with either low or middle cloudiness.

*Kaltenbach, J. L., ed., 1970: "Science Report on the 70-mm Photography of the Apollo 6 Mission", NASA—Manned Spacecraft Center Report S-217, Manned Spacecraft Center, Houston, Texas, 314 pp.

Table 13—Apollo 6 cloud type distribution for Apollo segment 1 after stereographic viewing. The cloud type percentages were computed in the same manner as in Table 11.

Low Cloudiness		Middle Cloudiness		High Cloudiness	
Cloud type	Percentage of total cloud cover	Cloud type	Percentage of total cloud cover	Cloud type	Percentage of total cloud cover
Sc	10.0	Ac	13.6	Ci	18.7
Sc, Ci	0.9	As	0.3	Cs	15.7
Cu	12.2	Ac, Cu	7.2	Thin Ci	2.7
Cu, Ci	0.8	Ac, few Cu	0.1	Thin Ci, Ac, few Cu	0.7
		Ac, Ci	0.3	Ci, few Cu	2.2
		Ac, few Ci	0.3	Ci, Cu	0.7
		Ac, Cu, few thin Ci	6.6	Ci, Ac	0.7
		Ac, few Cu, few Ci	1.2	Ci, Ac, Cu	0.3
		As, Cu	1.9	Cs, Cu	0.8
		As, few Ac, few Cu	0.7	Cs, Ac	1.4
Total = 23.9%		Total = 32.2%		Total = 43.9%	

Note: The total percentages for single, double, and triple layers are 73.2, 17.3, and 9.5, respectively.

The relabeling of cloud type from stratocumulus to altocumulus in frame 842 to 856 was the principal cause of the substantial increase (13.2 percent) in the middle cloud cover for segment 1. This is seen in Table 13 along with the rest of the new cloud type distribution which followed from the viewing of the stereographic pairs. Because the altocumulus deck was very low for middle clouds, the earlier conclusion that most of the clouds were near low levels or at high levels except those close to organized systems was still valid.

Among the changes made to the east of frame 856 was the relabeling of a cumulonimbus cloud type to cumulus and altocumulus beneath a cirrus canopy in frame 874. The canopy was detected after the stereographic view revealed considerable vertical separation between the cirrus and the clouds below.

The stereographic viewing also provided greater confidence in the judgments concerning the presence or absence of multilayered clouds. From Table 13 it is found that 73.2 percent of the clouds in segment 1 were in areas where only a single layer existed, or where there was a multiple layer in which the cloud elements were sufficiently separated to indicate individually each element of every layer along the cloud line. This result is in close agreement with the 70-percent cloud distribution in the single-level category noted before the stereographic viewing. Often there were clouds at different levels within one of the three major cloud levels. This was especially true for middle and high clouds. The multilayered cloud situations covered 26.8 percent of the total cloud distribution for segment 1 and were primarily located in the regions of the weakening stationary front and the more organized subtropical system near 27° N, 43° W.

New cloud type judgments made from viewing stereographic pairs were more common along the center line of segment 2 than for segment 1. Figure 18 shows the original and revised Apollo center

lines for frames 1464 to 1478 within segment 2. The surface weather observations at 1500 GMT were also used in determining the cloud types along the revised center line. In these center-line analyses of the cloudiness associated with the double cold front, the errors in cloud type that were made without the assistance of surface reports and stereographic viewing when many layers of clouds were present can be seen. As many as six cloud layers could be identified through a hole in the clouds near the location of one of the fronts. The most common mistake made in the original cloud line was the indication of middle cloud as the highest cloud layer when cirrus clouds were actually present. This error often led to another mistake of identifying a middle cloud as a low cloud since it appeared to be below the highest layer.

The substitution of stratocumulus for cumulus as the low cloud present was made from the surface observations. In most instances of multilayered clouds the lowest layer was not clearly visible over a large enough area to make a good cloud type determination from the prints or the stereographic pairs. This resulted in the incorrect choice of cumulus clouds for both. East of frame 1481, where the cloudiness from the fronts was no longer present, the cloud type judgments that had been made in the original cloud line were verified except in some very minor instances.

Table 14 depicts the revised cloud type distribution for segment 2. The greatest change which resulted from the stereographic viewing and surface reports was a sharp decrease in the percentage of middle clouds where they were predominant in a multilayered situation. This followed from the realization that what had been previously identified as combinations of middle and low cloud types were actually combinations of middle and high, and middle, high, and low types. Some cirrocumulus, generally considered to a rare cloud type, were observed in frame 1478 to 1479. The cirrocumulus could be positively identified only by stereographic viewing.

Table 14—Apollo 6 cloud type distribution for Apollo segment 2 after stereographic viewing and use of conventional data. The cloud type percentages were computed in the same manner as in Table 12.

Low Cloudiness		Middle Cloudiness		High Cloudiness	
Cloud type	Percentage of total cloud cover	Cloud type	Percentage of total cloud cover	Cloud type	Percentage of total cloud cover
Sc	30.6	Ac	3.8	Ci	0.9
Cu	11.0	Ac, Sc	2.9	Cs	17.8
Sc, Cu	4.2			Cb	2.2
				Ci, Cu	0.8
				Ci, Sc	9.0
				Ci, Ac	7.7
				Ci, Ac, Sc	2.9
				Cs, As	2.5
				Cs, Ac, Sc	1.3
				Cc, Ac, Sc	2.0
				Thin Ci	0.4
Total = 45.8%		Total = 6.7%		Total = 47.5%	
Note: The total percentages for single, double, and triple layers are 66.7, 27.1, and 6.2, respectively.					

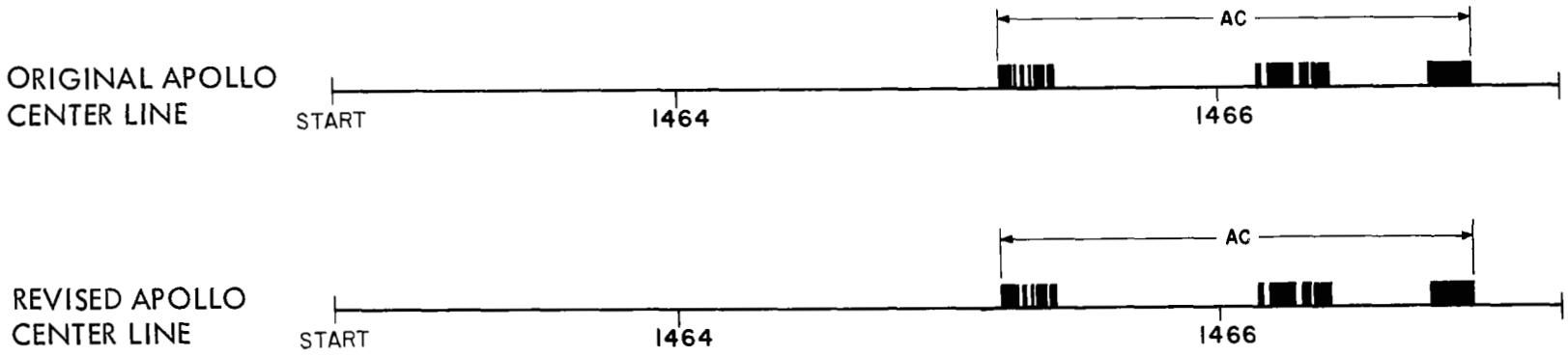
ORIGINAL APOLLO
CENTER LINE
START
1464
AC
1466
REVISED APOLLO
CENTER LINE
START
1464
AC
1466

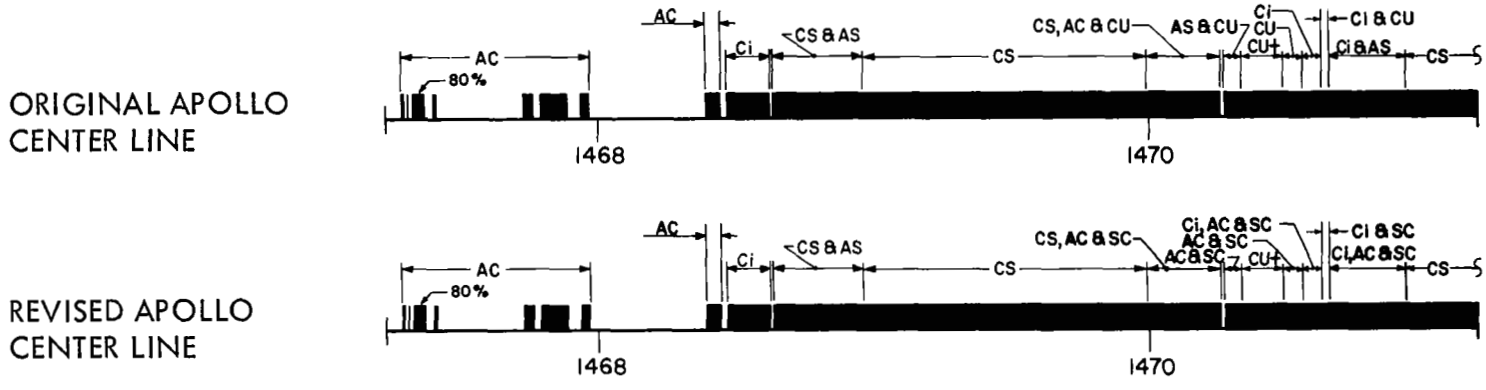
ORIGINAL APOLLO
CENTER LINE
AC
80%
AC
Ci
CS & AS
CS
CS, AC & CU
AS & CU
Ci
CU
CU+
Ci & CU
Ci & AS
CS
1468
1470
REVISED APOLLO
CENTER LINE
AC
80%
AC
Ci
CS & AS
CS
CS, AC & SC
Ci, AC & SC
AC & SC
AC & SC
CU+
Ci & SC
Ci, AC & SC
CS
1468
1470

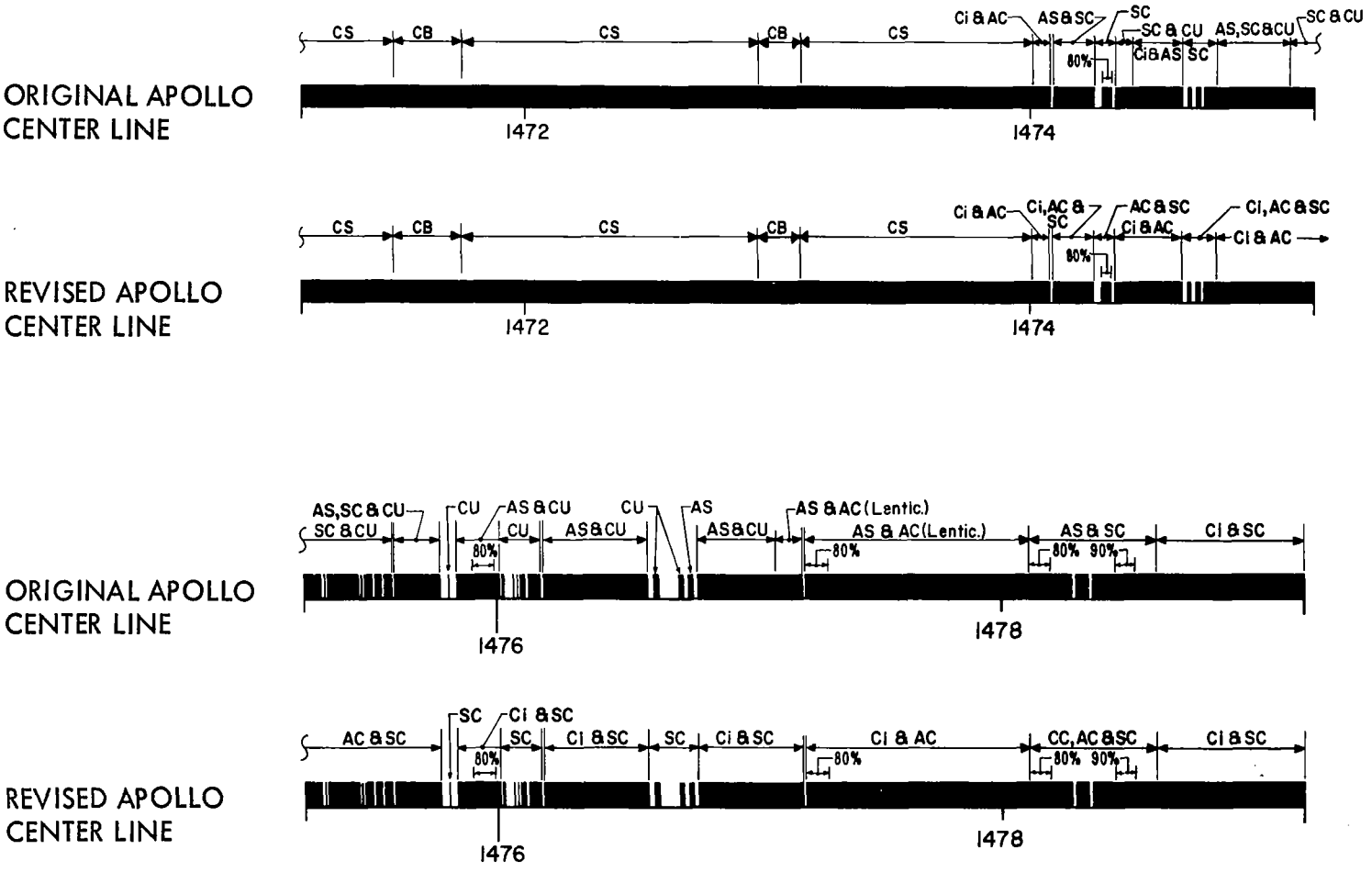

Figure 18—Original and revised (after stereographic viewing) Apollo 6 center-line data from Apollo 6 frame 1464 to frame 1478. The presentation of these data is the same as in Figure 2. The percentages of cloud cover indicated above the cloud blocks are for regions of broken cloud cover where the spacing was too small to show each cloud element.

A single layer of clouds was observed for 66.7 percent of the segment 2 cloud cover. Nearly all of the single layer cloud conditions occurred to the east of frame 1480, east of the cloudiness associated with the double cold front. The double and triple layers were associated almost exclusively with the double cold front.

7. CLOUD TYPE COMPARISONS BETWEEN APOLLO 6 AND ATS 3 MEASUREMENTS AND BETWEEN APOLLO 6 AND ESSA 3 MEASUREMENTS

To illustrate the similarities and differences of cloud type identification between the Apollo 6 and ATS 3 4X data, several regions were selected where the Apollo 6 pictures indicated relatively homogeneous cloud type conditions for a sizeable portion of the revised Apollo center line. Between Apollo 6 frames 836 and 856 the cloud types identified in the Apollo 6 pictures were either low altocumulus, stratocumulus, or cumulus. Both analysts generally agreed that the estimated cloud types from the ATS 3 photographs were cumuliform. Analyst 2 was more accurate than analyst 1 with the 4X pictures in that he indicated some altocumulus in frames 854 to 856, whereas analyst 1 indicated altocumulus for only a short distance in frame 848. No altocumulus was shown by either analyst for the 1X pictures. From Apollo 6 frame 856 to 860 and from 864 to 870 a combination of middle and low clouds associated with the weakening cold front predominated (Figure 2). Analyst 1 (using the Conover method) derived from the 4X pictures mostly multilayered cloud cover, which consisted mainly of stratocumulus, cumulus, nimbostratus, altostratus, and altocumulus. Analyst 2 identified mostly stratocumulus and altocumulus, with some altostratus for a short distance. Therefore, both analysts detected some evidence of multilayered cloud structure. The analysis of the 1X photographs showed that some discriminating capability was lost by analyst 2, who estimated only low cumuliform cloudiness, whereas analyst 1 still indicated multilayered structure.

The Apollo 6 cloud coverage between Apollo 6 frames 872 and 874 was an outstanding example of how the cloud distribution and structure could be detailed in the Apollo 6 pictures and how this detail was lacking in the ATS 3 data. Figure 19 shows the Apollo 6 center-line data and the concurrent ATS 3 data from just before the midpoint of Apollo 6 frame 872 to just after the midpoint of frame 874. The detail shown in the Apollo 6 cloud line is not present in the other cloud lines. Multilayered clouds were estimated by analyst 1 from the ATS 3 4X photograph, and there is no indication of cirrus given by either analyst for the 4X and 1X pictures: Figure 9 shows the extent of the cirrus clouds that were present in frame 873.

Apollo 6 frames 882 to 896 showed an extensive cloud shield associated with a subtropical system. The only evidence in the 1200 GMT surface analysis (Figure 6) that such a system could be present was a slight cyclonic circulation in the surface easterlies south of the center of the subtropical high-pressure system. There was no increase in the cyclonic curvature on the surface charts subsequent to the one at 1200 GMT. However, there was a well defined 500-mb trough at 1200 GMT (Figure 7) with a possible closed circulation at 29° N, 56° W. The trough weakened and within 24 hours the center of the circulation moved slowly south-southeastward to be located at 23° N, 54° W. It is likely that the subtropical disturbance was enhanced by the greater instability and cyclonic flow associated with this middle-tropospheric circulation. Extensive cirriform clouds were connected with the system, and occasionally low cumuliform and middle clouds could be seen below. Along portions of the Apollo 6 center line the dense cirrostratus prevented the viewing of any

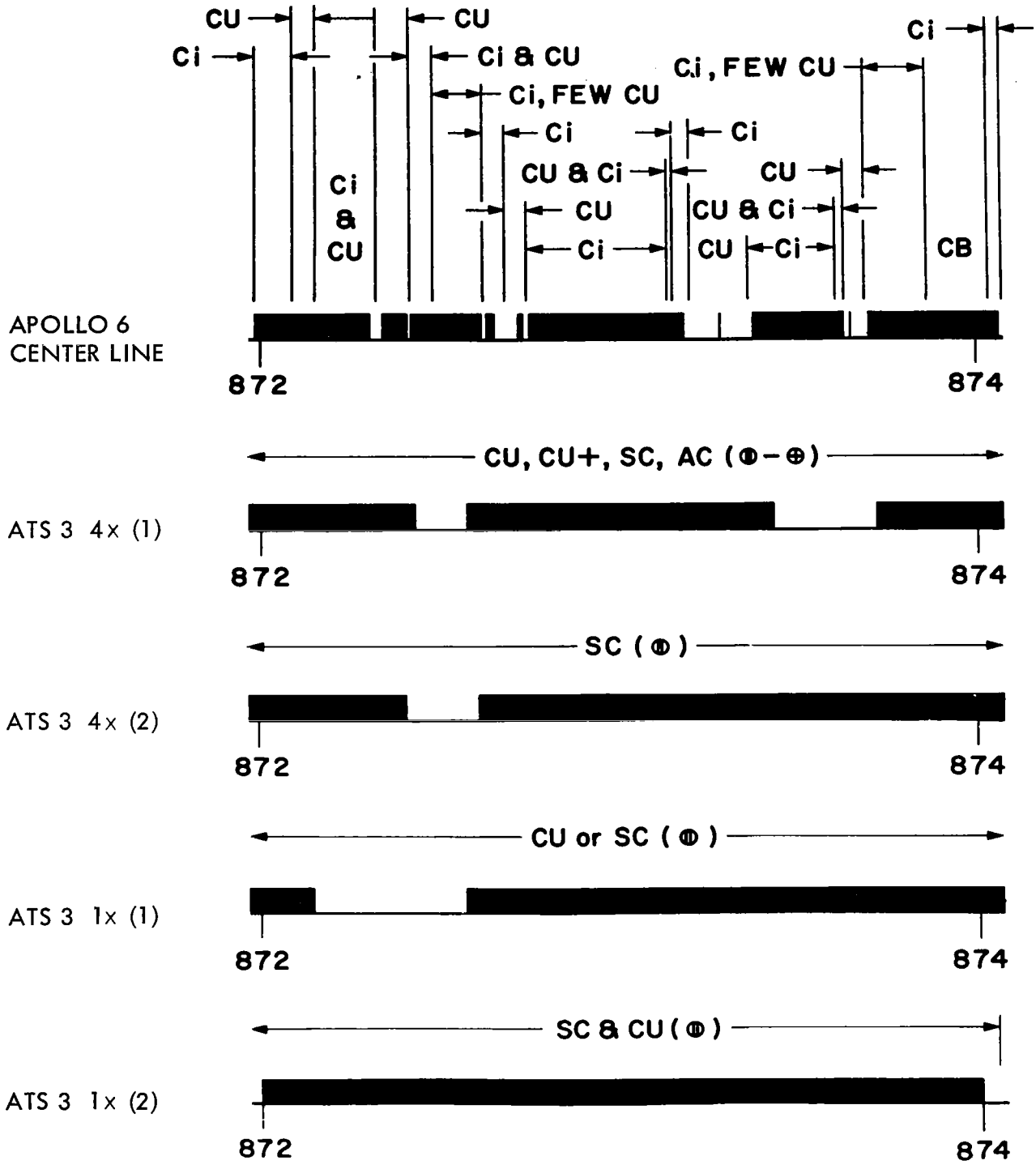

Figure 19—The cloud type and cover information along the center line of the Apollo 6 pictures, and the concurrent lines from the ATS 3 photographs for both analysts. The midpoints of the Apollo frame numbers are indicated below each cloud line. Areas filled completely by clouds are shown by the darkened portions.

possible low and middle clouds. The judgment of both analysts for the 4X data was that multilayered clouds were present over portions of the system between Apollo 6 frames 882 and 896. There was disagreement between the analysts with the 1X pictures; analyst 1 indicated multilayered clouds and analyst 2 only cumuliform clouds. This result was consistent with the cloud type determinations made in conjunction with the more organized system found in frame 856 to 860 and 864 to 870. The cloud type estimates from ESSA 3 frame 5 for this system were about the same as noted for the ATS 3 1X pictures.

Between Apollo 6 frames 896 and 928, the clouds were mostly low cumuliform. These clouds were often seen in short lines where small circulations were probably dominant and where there was no evidence from the cloud distributions of large-scale well-organized systems. The distributions from both analysts agreed that cumuliform cloud types predominated with the only discrepancies being an occasional estimate of middle or high clouds for a short distance.

From Apollo 6 frame 928 eastward to the West Coast of Africa in frame 935, large bands of cirrus clouds associated with a subtropical jet stream were the principal cloud type present. A few cumulus and a patch of altostratus were indicated beneath the cirrus. Neither analyst indicated continuous cirrus clouds for the ATS 3 and ESSA 3 measurements across these Apollo 6 frames. The principal cloud types were judged to be stratocumulus and cumulus.

The cloud type comparisons revealed that when low cumuliform clouds were present in the Apollo 6 pictures both analysts were quite accurate in their cloud type estimates. When multilayered cloudiness associated with well-organized systems become predominant, discrepancies began to appear between the two analysts, with the Conover method providing slightly more accurate estimates. However, this method did not always permit definitive decisions in situations where analyst 1 could not make a clear choice among cloud categories. When cirrus clouds were the principal cloud type present with little cloud activity below the cirrus level, both analysts experienced considerable difficulty with the cloud type decision. The cirrus were often mistakenly identified as cumuliform cloud types, and there were places where the cirrus clouds were undetectable, especially by the degraded ESSA 3 camera.

The cloud-type estimate results were similar for segment 2, with the greatest discrepancies occurring where the cloudiness was associated with the double cold front.

8. CONCLUSIONS

The high-resolution Apollo 6 photography has permitted the first concurrent comparison of routine satellite measurements with data that give a nearly perfect view of the cloud types and extent of cloud cover. It has also been possible to examine the significance of independent information on cloud height obtained through stereographic viewing of picture pairs for the two Apollo segments.

A substantial overestimation of the percentage of cloud cover occurred when the effects of spatial resolution and viewing perspective were not considered for the ATS 3 cloud measurements. The overestimations were made principally where cumuliform clouds were present, and approached a factor of 2 for this kind of cloudiness in both segments. When a viewing-perspective correction was applied, overestimations of the percentage of cloud cover from the ATS 3 data were reduced but were still about 10 percent too high. This would be expected for the ATS 3 data with no correction for

sensor spatial resolution when a digital method of estimating the cloud cover percentages is employed; such a method establishes a cloud/no-cloud brightness threshold at low brightness. Further somewhat subjective corrections were applied from experience for the spatial resolution effect and with a cloud cover model developed by Conover (1962, 1963). These, along with the perspective correction, produced reasonable agreement between the ATS 3 and Apollo 6 cloud cover percentages. The adjustment methods could be used over limited regions where detailed cloud cover information is required. However, to process large amounts of data in a more objective manner, digital procedures are necessary. Improvements in the estimates of cloud cover percentages by digital methods could be derived from increased sensor spatial resolutions, relationships of higher precision between brightness and cloud cover where calculations of cloud type and thickness are made, and more sophistication in the threshold techniques using normalized brightness measurements.

Sensor degradation was found to be extremely important in the determination of the percentage of cloud cover. Comparison of the ESSA 3 and Apollo 6 pictures showed that the percentages were underestimated for the former even before sensor spatial resolution and perspective corrections were considered. Also, a substantial underestimation was noted when an objective brightness technique developed by Miller et al. (1970) was employed. The underestimations were greatest when, due to insufficient instrument sensitivity, cirrus clouds were not detected. Therefore, cautious interpretation is necessary of cloud statistics acquired from sensors where degradation has occurred. It is important that data acquired from these sensors is not mixed with data received from better sensors because cloud cover anomalies noted during the length of record might be due to sensor characteristics rather than real differences in the percentage of cloud cover.

The cloud cover overestimates made from the ATS 3 satellite data (and also probably from conventional data) support the satellite earth-albedo determination of 30 percent, which is about 7 percent smaller than earlier albedo estimates made from conventional data.

It was possible to obtain cloud type distributions from the Apollo data in the subtropics and tropics as well as across a strong midlatitude cold front. The distributions indicated that middle clouds are generally associated only with organized systems whose cloud patterns have a characteristic scale size of at least 200 km. Middle clouds were also the least predominant (generally about 20 percent of the cloud types present), while with one exception, the remaining 80 percent were split about equally between high and low cloud types. The exception was the extensive region of low altocumulus noted between Apollo 6 frames 842 and 856 after viewing stereographic picture pairs of the region. Thus, the determination of wind from cloud motions in the subtropics and tropics will be principally from clouds at low and high levels, away from regions of organized systems.

The stereographic views of the clouds along the center lines of the two Apollo segments indicated that the cloud type decisions made along segment 1 were largely correct. However, extensive cloud type changes were suggested by viewing the stereographic picture pairs along the portion of segment 2 that traversed the double cold front in the Southeastern United States. Although the presence of more than one cloud layer was correctly identified from the Apollo 6 prints, specification of the cloud types that comprised the multiple layers was difficult. Often, cirrus occurring above one or more layers of clouds was either not detectable or incorrectly identified as a middle cloud type.

ACKNOWLEDGMENTS

The author appreciates the contributions of Lt. Col. John Hansen, Air Weather Service, United States Air Force, who participated in this study as the second analyst, and Major Donald Miller of the same organization, who supplied cloud-amount estimates from satellite brightness measurements.

Goddard Space Flight Center
National Aeronautics and Space Administration
Greenbelt, Maryland, December 31, 1970
160-44-51-01-51

REFERENCES

Appleman, H. S., 1962: "A Comparison of Simultaneous Aircraft and Surface Cloud Observations", *J. of Applied Meteor.* 1:548-551.

Barnes, J. C., 1966: "Note on the Use of Satellite Observations to Determine Average Cloudiness Over a Region", *J. of Geophys. Res.* 71:6137-6140.

Bertoni, E. A., 1970: "Clear Lines-of-Sight from Aircraft", Proceedings of the Fourth National Conference on Aerospace Meteorology, May 7-10, Las Vegas, Nevada.

Blackmer, R. H., Jr., E. J. Weigman, S. M. Serebreny, and R. G. Hadfield, 1970: "Analysis of ATS Photographs Using a Specially Designed Electronic Console", Stanford Research Institute, Menlo Park, California, Final Report, Phase 1, under Contract NAS5-21086, with NASA–Goddard Space Flight Center, Greenbelt, Maryland, 95 pp.

Conover, J. H., 1962: "Cloud Interpretation from Satellite Altitudes", AFCRL-62-680, Air Force Cambridge Research Laboratories, L. G. Hanscom Field, Bedford, Massachusetts, 77 pp.

Conover, J. H., 1963: "Cloud Interpretation from Satellite Altitudes", AFCRL-62-680, Supplement 1, Air Force Cambridge Research Laboratories, L. G. Hanscom Field, Bedford, Massachusetts, 19 pp.

Dines, W. H., 1917: "The Heat Balance of the Atmosphere", *Quarterly J. Roy. Meteor. Soc.* 43:151-158.

Environmental Data Service, 1967: "Catalog of Meteorological Satellite Data–ESSA 3 Television Cloud Photography, Part 2", ESSA–Meteorological Records Document 5.313, Environmental Science Services Administration, Washington, D.C., 29 pp.

Fox, R. L., 1961: "Sunshine-cloudiness relationships in the United States", *Mon. Weather Rev.* 89:543-548.

Fujita, T. T., 1970: "Basic Problems on Cloud Identification Related to the Design of SMS-GOES Spin Scan Radiometers", Research Paper 84, Univ. of Chicago SMRP, Chicago, Illinois, 33 pp.

Goddard Space Flight Center, 1968: "Meteorological Data Catalog for the Applications Technology Satellites", Vol. II, NASA Technical Memorandum X-66467, 353 pp.

Lund, I. A., 1965: "Estimating the Probability of Clear Lines-of-Sight from Sunshine and Cloud Cover Observations", *J. of Applied Meteor.* 4(6):714-722.

Lund, I. A., 1966: "Methods for Estimating the Probability of Clear Lines-of-Sight, or Sunshine, through the Atmosphere", *J. of Applied Meteor.* 5(5):625-630.

McCabe, J. T., 1965: "Estimating Mean Cloud and Climatological Probability of Cloud-Free Lines-of-Sight", Environmental Technical Applications Center Technical Report 186, United States Air Force, Washington, D.C., 26 pp.

Miller, D. B., R. E. Miller, and A. L. Booth, 1970: "An Automated Method of Estimating Total Cloud Amount from Meso-scale Satellite Data", Proceedings of the Symposium on Tropical Meteorology, June 2-11, 1970, Honolulu, Hawaii.

Raschke, E., and W. R. Bandeen, 1970: "The Radiation Balance of the Planet Earth from Radiation Measurements of the Satellite Nimbus II", *J. of Applied Meteor.* 9:215-238.

Schwalb, A. and J. Gross, 1969: "Vidicon Data Limitations", ESSA Technical Memo NESCTM 17, Environmental Science Services Administration, Washington, D.C., 22 pp.

Shenk, W. E., and V. V. Salomonson, 1971: "A Simulation Study Exploring the Effects of Sensor Spatial Resolution on Estimates of Cloud Cover from Satellites", NASA Technical Note D-6247, 18 pp.

Stamm, A. J., and T. H. Vonder Haar, 1970: "A Study of Cloud Distributions Using Reflected Radiance Measurements from the ATS Satellites", *J. of Applied Meteor.* 9:498-507.

Whitehead, V. S., I. D. Browne, and J. G. Garcia, 1969: "Cloud Height Contouring from Apollo 6 Photography", *Bull. of the Amer. Meteor. Soc.* 50:522-528.

World Meteorological Organization, 1956: "International Cloud Atlas", Vol. I and II, World Meteorological Organization, Geneva, Switzerland.

Young, M. J., 1967: "Variability in Estimating Total Cloud Cover from Satellite Pictures", *J. of Applied Meteor.* 6(3):573-579.

NASA-Langley, 1971 —— 20

"The aeronautical and space activities of the United States shall be conducted so as to contribute . . . to the expansion of human knowledge of phenomena in the atmosphere and space. The Administration shall provide for the widest practicable and appropriate dissemination of information concerning its activities and the results thereof."

—NATIONAL AERONAUTICS AND SPACE ACT OF 1958

NASA SCIENTIFIC AND TECHNICAL PUBLICATIONS

TECHNICAL REPORTS: Scientific and technical information considered important, complete, and a lasting contribution to existing knowledge.

TECHNICAL NOTES: Information less broad in scope but nevertheless of importance as a contribution to existing knowledge.

TECHNICAL MEMORANDUMS: Information receiving limited distribution because of preliminary data, security classification, or other reasons.

CONTRACTOR REPORTS: Scientific and technical information generated under a NASA contract or grant and considered an important contribution to existing knowledge.

TECHNICAL TRANSLATIONS: Information published in a foreign language considered to merit NASA distribution in English.

SPECIAL PUBLICATIONS: Information derived from or of value to NASA activities. Publications include conference proceedings, monographs, data compilations, handbooks, sourcebooks, and special bibliographies.

TECHNOLOGY UTILIZATION PUBLICATIONS: Information on technology used by NASA that may be of particular interest in commercial and other non-aerospace applications. Publications include Tech Briefs, Technology Utilization Reports and Technology Surveys.

Details on the availability of these publications may be obtained from:

SCIENTIFIC AND TECHNICAL INFORMATION OFFICE

NATIONAL AERONAUTICS AND SPACE ADMINISTRATION

Washington, D.C. 20546